

Sexually Dimorphic Neurons in the Ventromedial Hypothalamus Govern Mating in Both Sexes and Aggression in Males

Cindy F. Yang,^{1,2} Michael C. Chiang,² Daniel C. Gray,³ Mahalakshmi Prabhakaran,² Maricruz Alvarado,² Scott A. Juntti,^{1,6} Elizabeth K. Unger,⁴ James A. Wells,^{3,5} and Nirao M. Shah^{1,2,4,*}

¹Program in Neuroscience

²Department of Anatomy

³Program in Chemistry and Chemical Biology

⁴Program in Biomedical Sciences

⁵Departments of Pharmaceutical Chemistry and Cellular and Molecular Pharmacology

University of California, San Francisco, San Francisco, CA 94158, USA

⁶Present address: Department of Biology, Stanford University, Stanford, CA 94305, USA

*Correspondence: nms@ucsf.edu

<http://dx.doi.org/10.1016/j.cell.2013.04.017>

SUMMARY

Sexual dimorphisms in the brain underlie behavioral sex differences, but the function of individual sexually dimorphic neuronal populations is poorly understood. Neuronal sexual dimorphisms typically represent quantitative differences in cell number, gene expression, or other features, and it is unknown whether these dimorphisms control sex-typical behavior exclusively in one sex or in both sexes. The progesterone receptor (PR) controls female sexual behavior, and we find many sex differences in number, distribution, or projections of PR-expressing neurons in the adult mouse brain. Using a genetic strategy we developed, we have ablated one such dimorphic PR-expressing neuronal population located in the ventromedial hypothalamus (VMH). Ablation of these neurons in females greatly diminishes sexual receptivity. Strikingly, the corresponding ablation in males reduces mating and aggression. Our findings reveal the functions of a molecularly defined, sexually dimorphic neuronal population in the brain. Moreover, we show that sexually dimorphic neurons can control distinct sex-typical behaviors in both sexes.

INTRODUCTION

Males and females show sex differences in many behaviors, including mating and aggression, that result from sexually dimorphic development or the activation of underlying neural circuits. Gonadal sex hormones exert a profound influence on vertebrate sex-typical behaviors by controlling sex differences in the brain (Cooke et al., 1998; Dewing et al., 2003; Gagnidze et al., 2010;

Jazin and Cahill, 2010; McCarthy and Arnold, 2011; Morris et al., 2004; Simerly, 2002; De Vries, 1990; Xu et al., 2012; Yang et al., 2006). Most behaviors and neural circuits are shared between the sexes such that sexually dimorphic neuronal clusters represent a small fraction of the neurons within larger brain regions. Therefore, it has been difficult to discern which dimorphic, hormone-responsive neurons in the brain control each of the various sex differences in physiology and behavior. In addition, neuronal sex differences usually represent quantitative rather than all-or-nothing dimorphisms in gene expression or cytological features. Presently, it is unclear whether such groups of dimorphic neurons regulate gender-typical behaviors in one or both sexes.

Progesterone controls female reproduction, including sexual receptivity, by signaling via its cognate receptor (progesterone receptor [PR]) (Levine et al., 2001; Mani et al., 1997). PR is widely distributed in the brain, and the PR+ neurons that regulate sexual receptivity have yet to be identified unambiguously (Blaustein and Feder, 1979; Olster and Blaustein, 1990; Quadros et al., 2008). The ventromedial hypothalamus (VMH), which contains a small pool of PR+ neurons in its ventrolateral division (VMHvl), is well characterized for its relevance to female mating in mammals (Blaustein, 2008; Cohen and Pfaff, 1992; Flanagan-Cato, 2011; Rubin and Barfield, 1983). Studies with c-Fos suggest that many VMHvl neurons, including a subset of PR+ neurons, are activated after female mating (Flanagan-Cato et al., 2006). However, lesions or manipulations of neuronal activity of the VMH can lead to no change, decrease, or increase in female sexual behavior (Goy and Phoenix, 1963; Kow et al., 1985; Leedy and Hart, 1985; Mathews and Edwards, 1977a, 1977b; Musatov et al., 2006; Pfaff and Sakuma, 1979a, 1979b; Robarts and Baum, 2007; La Vaque and Rodgers, 1975). Some studies also report a concurrent increase in body weight, suggesting a complex role of this region in feeding and mating (King, 2006; Musatov et al., 2007). This phenotypic diversity is most likely due to manipulations that variably affect the heterogeneous neuronal subsets within the VMH (Kurrasch et al., 2007), adjacent brain

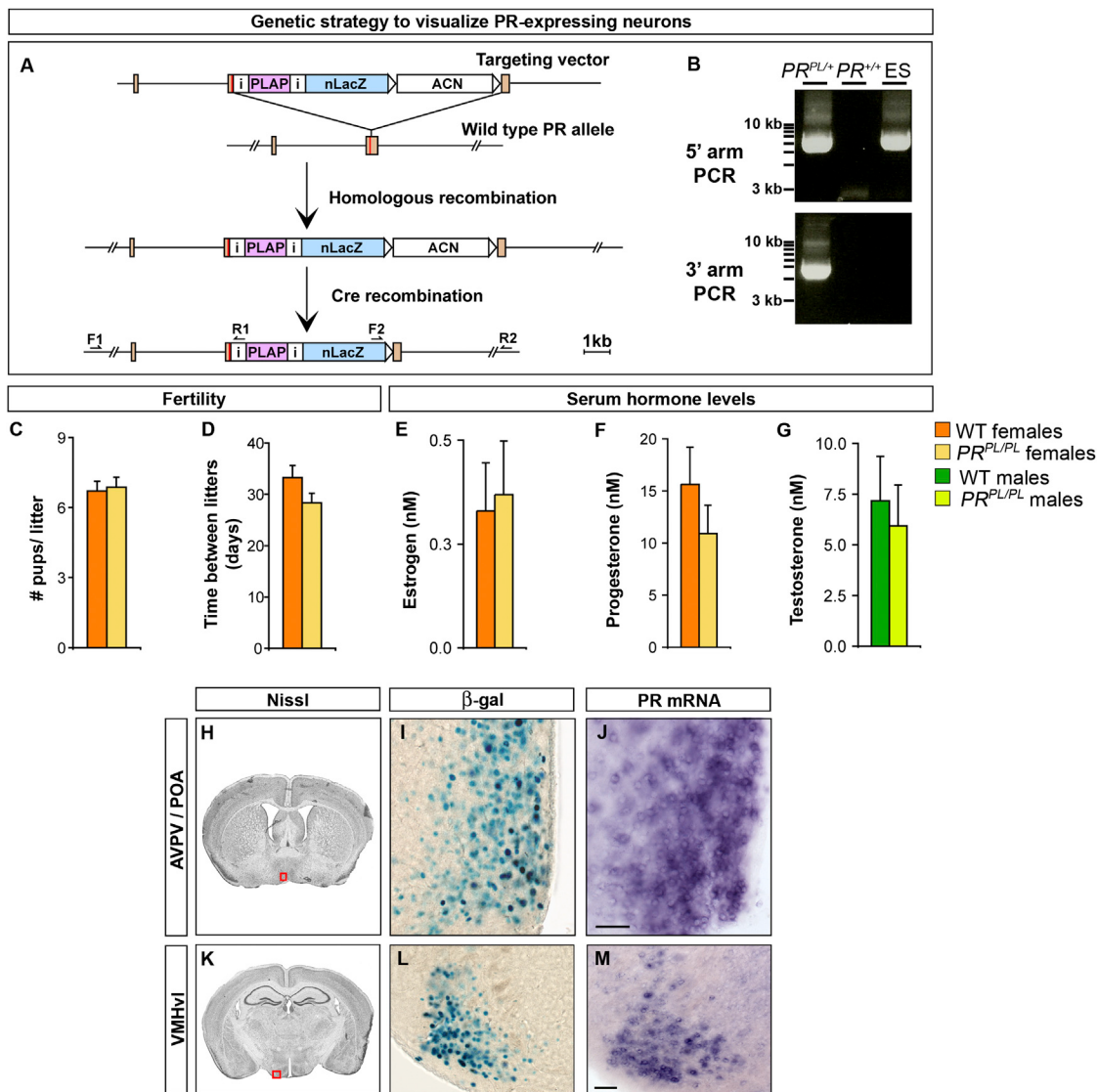


Figure 1. Visualizing PR+ Neurons in the Mouse Brain

(A) The generation of the *PR^{PL}* allele. ACN is a self-excising neomycin-selection cassette (Bunting et al., 1999). Orange rectangles represent exons, and the red line in the 3' exon denotes the stop codon.

(B) PCR was performed in order to detect homologous recombination at the *PR* locus. Primers were used to detect integration of the 5' (F1 and R1) and 3' (F2 and R2) arms of the targeting vector. ACN precludes detection of the 3' recombination event in embryonic stem (ES) cells.

(C and D) There was no difference between WT and *PR^{PL/PL}* females in litter size and frequency.

(E–G) There was no difference in titers of sex hormones between WT and *PR^{PL/PL}* adults.

(H–M) Boxed areas in Nissl-stained coronal sections (Paxinos and Franklin, 2003) through the adult brain depict locations of the regions shown in panels to the right. PR expression in *PR^{PL/+}* female as labeled by β -gal activity mirrors the expression of PR mRNA in adjacent sections.

Scale bars represent 50 μ m. Mean \pm SEM; $n \geq 12$ per genotype (C–G); $n = 3$ (H–M).

Also see Figure S1 and Table S3.

regions, and fibers of passage. Given these challenges, the identity and function of VMHvl neurons that specifically influence female mating remain unclear.

In accord with the notion that the VMHvl influences female sexual behavior, the VMHvl exhibits quantitative cell and molecular sex differences (Dugger et al., 2007; Grgurevic et al., 2012; Matsumoto and Arai, 1983, 1986; Patisaul et al., 2008; Wu et al., 2009; Xu et al., 2012). In addition, lesions or

manipulations of neural activity of the VMH or the surrounding neurons have long suggested an important role of this region in controlling aggression (Hess and Akert, 1955; Kruk et al., 1979; Reeves and Plum, 1969; Wheatley, 1944). In fact, this region is activated during male aggression, and, correspondingly, electrical activation or inhibition of this region elicits or inhibits fighting, respectively (Kollack-Walker and Newman, 1995; Lin et al., 2011; Veening et al., 2005). However, as with VMH neurons that

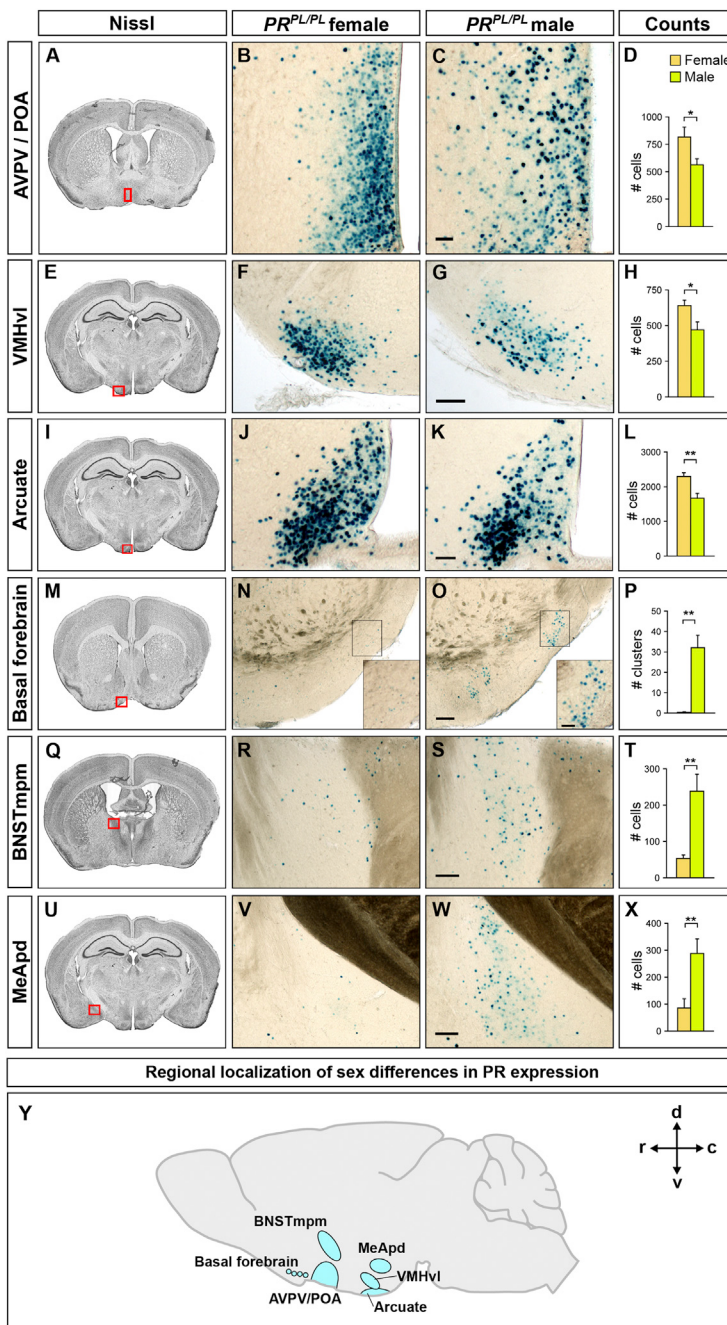


Figure 2. Sexual Dimorphism in PR Expression in the Adult Brain

Boxed areas in Nissl-stained coronal sections through the adult brain depict regions of $PR^{PL/PL}$ mice labeled for β -gal activity in the panels to the right.

(A–L) More PR+ cells are present in the female AVPV and POA, VMHvl, and arcuate nucleus.

(M–X) More PR+ cells are present in the male basal forebrain, BNSTmpm, and MeApd.

(Y) A representation of sexually dimorphic PR expression in different brain regions as projected on to a midsagittal section. c, caudal; d, dorsal; r, rostral; and v, ventral.

Scale bars represent 50 μ m (C and K) and 100 μ m (G, O, S, and W). The inset scale bar represents 25 μ m. Mean \pm SEM; n \geq 4 per sex. *, p < 0.04; **, p < 0.01.

Also see Figure S2 and Table S1.

this approach, we have ablated PR+ VMHvl neurons in adult females, and we observe a dramatic reduction in sexual receptivity. The corresponding ablation in males reduces mating and territorial aggression. Thus, our results define a role of PR+ VMHvl neurons in sex-typical behaviors. Moreover, we establish that a discrete, sexually dimorphic neuronal population influences sexually dimorphic behaviors in both sexes.

RESULTS

Visualizing PR Expression in the Mouse Brain

We wished to identify PR+ neurons at high cellular resolution. We inserted an *IRES-PLAP-IRES-nuclear LacZ (PL)* reporter into the 3' untranslated region (UTR) of *PR* using gene targeting (Figures 1A and 1B). As described previously (Shah et al., 2004), this cassette permits the expression of placental alkaline phosphatase (PLAP), which labels neuronal processes, and nuclear targeted β -galactosidase (β -gal) in PR+ cells. This strategy maintains the expression and function of PR and permits the examination of PR+ neurons in otherwise wild-type (WT) mice. Accordingly, and in contrast to $PR^{-/-}$ mice (Chappell et al., 1997; Lydon et al., 1995), $PR^{PL/PL}$ females were similar to WT females in fecundity and also maintained normal sex hormone titers (Figures 1C–1G).

In the forebrain, we observed β -gal activity in pools of neurons in specific hypothalamic nuclei, postero-dorsal medial amygdala (MeApd), medial division of the posteromedial bed nucleus of the stria terminalis

(BNSTmpm), various cortical areas, basal ganglia, and the dentate gyrus (Figures 1H–1M and 2; Figure S1 available online). This distribution of cells mirrors the expression pattern of PR messenger RNA (mRNA) in adjacent sections (Figures 1H–1M). In regions such as the basal ganglia, which have low-level PR expression that precludes visualization by *in situ* hybridization, we can detect PR message by quantitative RT-PCR (qRT-PCR) (Figure S1A). The distribution of β -gal+ cells was in accord with histological and pharmacological studies (Becker, 1999; Blaustein and Feder, 1979; Olster and Blaustein, 1990; Quadros

regulate female receptivity, the identity of the VMH neurons that influence aggression is unknown. In principle, these behaviors may be regulated by a single set of neurons or by nonoverlapping sets of neurons.

We utilized genetic strategies in mice to visualize PR+ neurons and to assess their contributions to mating and aggression. We find many sex differences in PR+ neurons in the adult brain, including in the VMHvl. We have developed a Cre-loxP strategy to ablate any molecularly defined neuronal population via targeted viral delivery of a genetically engineered caspase. Using

et al., 2008). In the case of the basal ganglia, our studies localized PR expression to sparsely distributed neurons across the rostro-caudal axis (Figures S1B–S1D). In addition, we found previously unreported PR+ neuronal pools scattered within the basal forebrain (Figure 2), an observation confirmed by qRT-PCR from this region (Figure S1A). The ~1 week $t_{1/2}$ of β -gal in neurons precluded detection of PR mRNA changes across the 4–6 day estrous cycle (Allen, 1922; Smith et al., 1995). However, the long $t_{1/2}$ and superb signal-to-noise ratio of β -gal labeling allowed for sensitive detection of PR expression. Altogether, the PR^{PL} reporter mouse confirmed and extended previous reports of PR expression in the mouse brain.

Widespread Sex Differences in the Distribution and Cell Number of PR+ Neurons

We observed previously unreported, as well as known, sex differences in PR+ cells in the adult PR^{PL} brain (Figures 2 and S2A and Table S1). We found more PR+ cells in the female pre-optic area (POA), the adjacent anteroventral periventricular hypothalamic nucleus (AVPV), arcuate nucleus, and VMHvl (Figures 2A–2L). The VMHvl contains cells expressing the estrogen receptor alpha (ER α or Esr1) (Xu et al., 2012), and we find that >92% PR+ neurons colabel for ER α in both sexes (Figure S2B). We asked whether PR+ VMHvl neurons expressed Cckar, a G protein-coupled receptor required for sexual receptivity and expressed in the female but essentially absent in the male VMHvl (Xu et al., 2012). We observed that $67\% \pm 3$ (mean \pm SEM) of PR+ VMHvl cells colabeled with Cckar, whereas $96\% \pm 0.2$ of Cckar+ VMHvl cells were PR+ ($n = 3$ $PR^{PL/PL}$ females, ≥ 500 cells analyzed per brain) (Figures S2C–S2E). Thus, PR+ neurons represent the vast majority of VMHvl neurons that express Cckar, a gene required for female mating.

We observed many clusters of PR+ cells (~15–40 cells per cluster) in the male, but not the female, basal forebrain (Figures 2M–2P). Along with a sex difference in androgen receptor expression in this region (Shah et al., 2004), our findings suggest an unappreciated role of the basal forebrain in responding to sex hormones. We also found more PR+ cells in the male BNSTmpm and MeApd (Figures 2Q–2X). This increased PR expression was surprising because there is little circulating progesterone in males; nevertheless, our findings are consistent with studies indicating a role of PR in male behaviors (Phelps et al., 1998; Schneider et al., 2005, 2009; Witt et al., 1995). As suggested previously (Mani et al., 1994a; Power et al., 1991; Tsutsui, 2012), PR may function in a progesterone-independent manner, or locally synthesized progesterone may activate PR in males. Consistent with these sex differences in PR expression, the POA, BNSTmpm, MeApd, arcuate nucleus, and VMHvl have been implicated in sex differences in behavior or physiology (Cooke et al., 1998; Morris et al., 2004; Simerly, 2002), and PR+ neurons in these regions could contribute to such sexually dimorphic output.

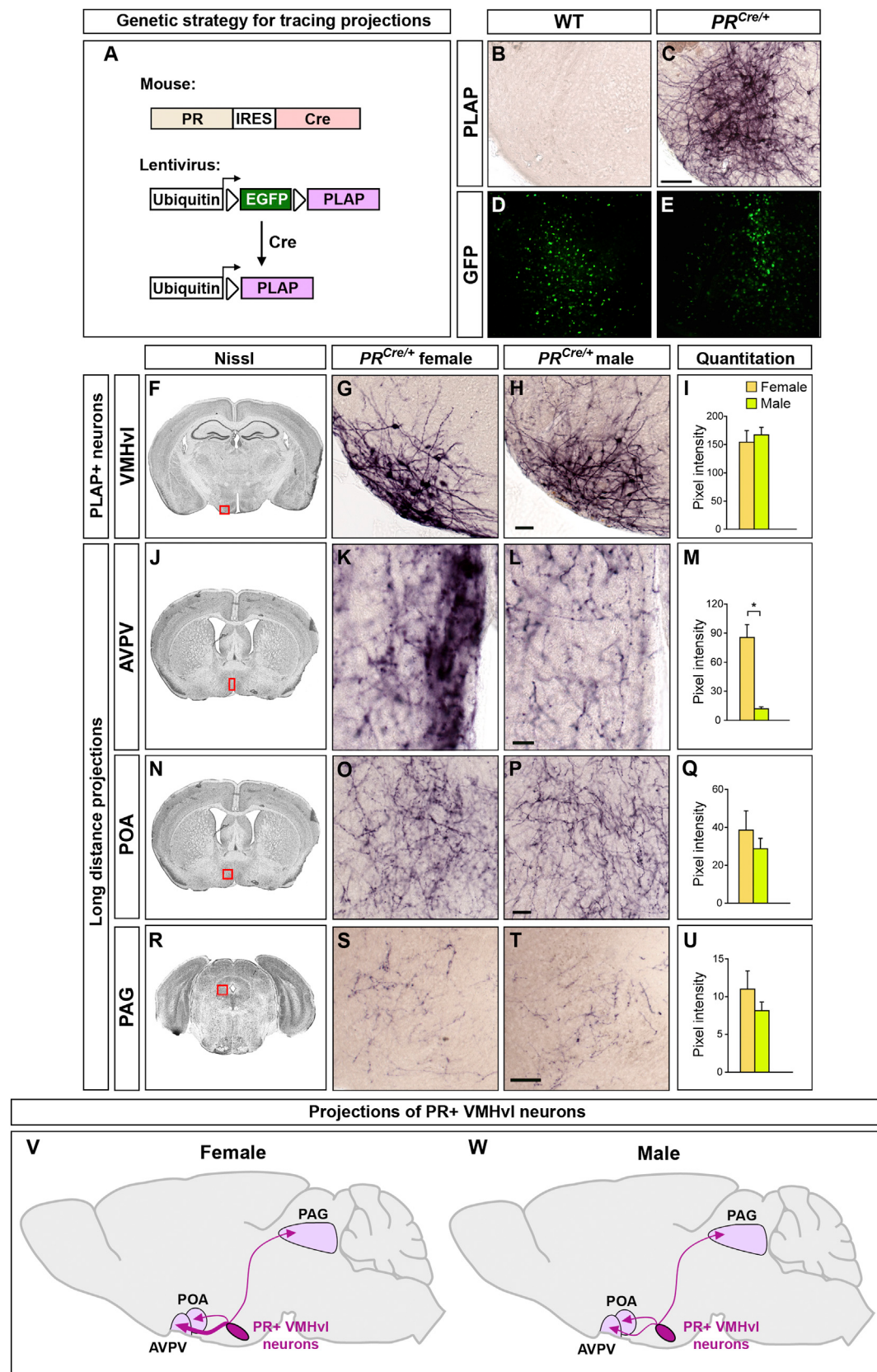
We find that the dimorphic PR+ cells colabel with pan-neuronal markers (Figure S2F). However, within any given brain region expressing PR dimorphically, only a subset of neurons is PR+. Even within the VMHvl, only $49\% \pm 4$ of NeuN+ cells colabel with PR ($n = 3$ brains, $\geq 10^3$ NeuN+ cells analyzed for PR per brain). There is a sex difference in the soma size of

thionin-labeled neurons within the rat VMHvl (Dugger et al., 2007). However, there was no such sex difference in PR+ VMHvl neurons (Figure S2G), suggesting either a species difference or that other VMHvl neurons account for this dimorphism. The sex differences in PR expression cannot result solely from sex differences in neuronal numbers. Indeed, no sex difference in neuronal number has been reported in the basal forebrain or VMHvl, and, in the POA and arcuate nucleus, which contain more neurons in males (Gorski et al., 1980; Leal et al., 1998), we found more PR+ neurons in females. Finally, the 3- to 4-fold more PR+ neurons in the male BNSTmpm and MeApd exceeds the <2-fold more neurons in these regions in males (Morris et al., 2008; Shah et al., 2004; Wu et al., 2009). Thus, our studies confirm known sex differences (POA, VMHvl, arcuate nucleus, and MeApd) (Blaustein et al., 1980; Brown et al., 1996; Grgurevic et al., 2012; Kudwa et al., 2009; Quadros et al., 2002) and reveal previously unreported sexual dimorphisms in PR expression (basal forebrain and BNSTmpm) in the mammalian brain.

Visualizing Sex Differences in Projections of PR+ Neurons

We determined whether sexually dimorphic PR+ neurons projected to distinct locations in the two sexes. Consistent with PR expression in interconnected regions such as the POA, BNST, MeA, and VMHvl, we observed a rich distribution of PLAP+ fibers in the $PR^{PL/PL}$ forebrain (data not shown) that precluded the identification of dimorphic projection patterns. We devised a genetic strategy to visualize the projections of any subset of PR+ neurons. First, we targeted an IRES-Cre recombinase cassette to the 3' UTR of PR (Figures 3A, S3A, and S3B). As expected, these PR -IRES-Cre (PR^{Cre}) mice, like PR^{PL} mice, were viable and fertile, and Cre expression mirrored the expression of PR in the brain (Figures S3C–S3F). We also designed a lentiviral vector that expressed PLAP in a Cre-dependent manner (Lenti-Ixlplap; Figures 3A and S3G). This lentivirus is replication-incompetent and integrates into the host genome, properties that restrict PLAP expression to Cre+ cells for the life of the cells. This virus infects cells in both WT and PR^{Cre} mice, but we only observed PLAP expression in PR^{Cre} mice (Figures 3B–3E).

The VMH has been implicated in sex-specific behaviors, and, therefore, we traced the projections of PR+ VMHvl neurons in adults. Initially, we determined that we could visualize maximal expression of PLAP 7–8 days following the delivery of Lenti-Ixlplap into the VMH (C.F.Y., unpublished data). Such injections revealed the soma and local arbor of PR+ VMHvl neurons (Figures 3F–3I). In contrast to the wide-ranging projections of the entire VMH (Saper et al., 1976; Krieger et al., 1979), we observed PLAP+ projections of PR+ VMHvl neurons in the AVPV and adjacent periventricular area, POA, and periaqueductal gray (PAG) (Figures 3J–3U). Unlike PR+ VMHvl projections in the guinea pig (Ricciardi and Blaustein, 1994), mouse PR+ VMHvl neurons did not appear to project appreciably to the BNST or MeA, suggesting subtle species differences in these cells. Although we observed a similar localization of PLAP+ projections of PR+ VMHvl neurons in both sexes (Figures 3J–3W and S3H and Table S2), there was a striking, previously unreported 7-fold increase in PLAP+ fibers in the female AVPV (Figures 3J–3M). This sex



(legend on next page)

difference cannot solely result from the dimorphism (~30%) in PR+ VMHvl cell number. In fact, we even observed the dimorphic AVPV projection in *PR^{Cre}* females in whom only a few PR+ VMHvl neurons had been infected. Thus, more PR+ female VMHvl neurons project to the AVPV, or their axonal termini arborize more extensively. The AVPV is thought to control ovulation, and the PAG can regulate sexual receptivity in females (Sakuma and Pfaff, 1979; Simerly, 2002). In summary, PR+ VMHvl neurons project to a subset of VMH targets, their efferents are sexually dimorphic, and each of their targets can influence sexually dimorphic behaviors or physiology.

A Genetic Approach to Ablate Adult Neurons In Vivo

We determined the requirement of PR+ VMHvl neurons in sex-typical behaviors by targeting Cre-dependent, virally encoded toxins to the VMHvl of *PR^{Cre}* mice. Initial studies suggested that virally encoded diphtheria toxin A or tBid (Jiang and Wang, 2004; Maxwell et al., 1986) were partially effective in ablating PR+ neurons in vivo, even though they were effective in tissue culture cells (C.F.Y., unpublished data). Therefore, we employed a genetically engineered caspase 3, a caspase whose activation commits a cell to apoptosis, in order to kill adult neurons in vivo (Figure 4A) (Gray et al., 2010). Endogenous caspase 3 normally exists as pro-caspase 3, and apoptotic signals activate upstream caspases that cleave pro-caspase 3 into its active form (Figure 4A). Our designer pro-caspase 3 (pro-taCasp3) lacks the cleavage site for upstream caspases and encodes a cleavage site for the heterologous enzyme tobacco etch virus protease (TEVp). Provision of TEVp activates pro-taCasp3 into the apoptosis-inducing taCasp3. We generated an adeno-associated virus (AAV) to drive the expression of pro-taCasp3 and TEVp in a Cre-dependent manner (Figures 4B and S4A) (Atasoy et al., 2008). This virus (AAV-flex-taCasp3-TEVp) utilizes the T2A peptide-encoding sequence to ensure bicistronic expression of pro-taCasp3 and TEVp. Importantly, taCasp3 triggers cell-autonomous apoptosis, thereby minimizing toxicity to adjacent non-Cre+ cells (Gray et al., 2010).

Infection of HEK293T cells with this virus led to rapid Cre-dependent cell death (Figures 4C–4D). Next, we tested whether this virus could ablate adult PR+ neurons by stereotactically targeting the virus to the VMHvl of adult *PR^{+/PL}* or *PR^{Cre/PL}* mice. PR+ VMHvl neurons appeared unaffected in controls but were essentially completely lost in *PR^{Cre/PL}* mice 2–4 weeks following viral delivery (Figures 4E, 4F, and S4B). We tested whether the

taCasp3-encoding AAV targeted to the VMHvl diffused to and ablated PR+ cells in distant hypothalamic regions. Therefore, we enumerated PR+ cells along the rostrocaudal extent of the hypothalamus in a cohort of virally injected control and *PR^{Cre}* mice. This analysis revealed no difference in PR+ cell counts between *PR^{Cre}* and control females (number of PR+ cells: control, 619 ± 60 and *PR^{Cre}*, 679 ± 150 ; n = 5 per cohort, p = 0.7). Thus, taCasp3-mediated ablation appears restricted to the vicinity of the injection site. We observed local spread of the virus to the arcuate, and we present these findings below. In separate experiments, we found that stereotaxic delivery of the taCasp3-encoding virus ablated Cre+ neurons in different brain regions (C.F.Y., E.K.U., and M.C.C., unpublished data), indicating that we have devised a general strategy for targeted ablation of Cre+ cells.

The Dimorphic PR+ VMHvl Cluster of Neurons Regulates Female Sexual Behavior

We tested the role of PR+ VMHvl neurons in female mating. We targeted AAV-flex-taCasp3-TEVp bilaterally to the VMHvl of adult *PR^{Cre}* and control females (Figure 5A). To assure optimal sexual receptivity, females were ovariectomized at the time of viral injection and, following recovery, hormonally primed to be in estrus when tested with WT males.

We observed a marked diminution of female sexual behavior in such *PR^{Cre}* females (Figures 5B–5G and Movies S1 and S2). As in many vertebrates, female mating in mice is stereotyped and includes permitting the male to approach and mount and dorsiflexing the neck and back (lordosis) upon sensory stimulation to the dorsum (Harvey, 1651; McGill, 1962). This allows males to intromit (penetrate, as determined by his thrust pattern) and attempt ejaculation. *PR^{Cre}* females rejected mount attempts by kicking or running away (Figure 5B), thereby reducing the fraction of mounts that progressed to intromission (receptivity index, Figure 5C). In sharp contrast to controls, *PR^{Cre}* females walked around during intromission, lordosed rarely, and showed a >20-fold reduction in lordosis duration (Figures 5D–5F). This reduced sexual behavior of *PR^{Cre}* females affected the WT male partner's performance (Figures 5H–5J). Males were interested in both *PR^{Cre}* and control females, initiating anogenital sniffing, mounting, and intromission equivalently but were less successful in ejaculating with the former (Figures 5H, S5A, and S5B). Accordingly, males intromitted only briefly with *PR^{Cre}* females, even though they mounted the females more and for

Figure 3. PR+ VMHvl Neurons Project in a Sexually Dimorphic Manner

(A) A strategy to visualize projections of PR+ neurons.

(B–E) Lenti-Ixplap targeted to the VMH infects cells in *PR^{Cre/+}* and WT mice, as visualized by EGFP+ cells. Only a few cells are PR+ in this region, so there is no apparent difference in the number of EGFP+ cells in *PR^{Cre}* and WT mice. PLAP+ soma and local arbors of VMHvl neurons are only observed in *PR^{Cre}* mice. (F–U) Boxed areas in Nissl-stained coronal sections depict regions shown in the panels to the right. Lenti-Ixplap targeted to the VMHvl of adult *PR^{Cre/+}* mice labels PLAP+ soma and local arbors of VMHvl neurons (F–I). The lentiviral titer limits the number of infected Cre+ neurons and does not highlight the sex difference in the number of these neurons. The variable multiplicity of infection can lead to apparent size differences in PLAP-labeled soma. However, there is no sex difference in the soma size of these neurons (Figure S2G). PR+ VMHvl neurons project to the AVPV, POA, and PAG (J–U). There are more PLAP+ projections to the AVPV in females (J–M) than to that in males.

(V and W) Shown is a schematic summarizing the projections of PR+ VMHvl neurons. No difference in the anatomical extent of projections in different regions were observed, but the female AVPV receives more innervation from these neurons.

Scale bars represent 100 μm (C), 50 μm (H, P, and T), and 25 μm (L). Mean \pm SEM; n \geq 7 per sex; *, p < 0.001.

Also see Figure S3 and Tables S2 and S3.

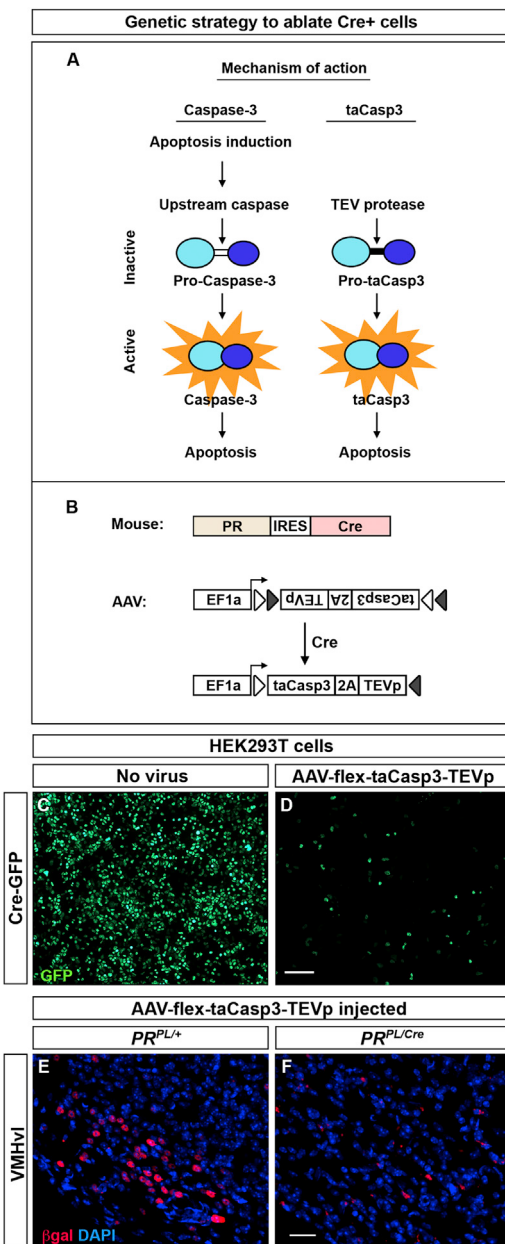


Figure 4. Genetic Strategy to Ablate Neurons in a Cre-Dependent Manner

(A) The intramolecular cleavage of endogenous pro-caspase 3 by upstream caspases activates caspase 3, which then induces apoptosis. This intramolecular cleavage site has been replaced by a TEV-linker domain (black bar) in inactive taCasp3 (pro-taCasp3) such that only TEV protease activates taCasp3, which then induces apoptosis.

(B) A genetic strategy to ablate PR+ neurons conditionally.

(C and D) Cell death 1 week following infection of Cre:EGFP+ HEK293T cells with AAV-flex-taCasp3-TEVp. n = 3 experiments.

(E and F) Ablation of PR+ VMHvl neurons in PR^{PL/Cre}, but not PR^{PL/+}, females injected with AAV-flex-taCasp3-TEVp. n ≥ 10 per experimental group.

The scale bar represents 100 μm (C and D) and 25 μm (E and F).

Also see Figure S4.

a longer duration (Figures 5I–5J). Correspondingly the total duration of intromission per assay was also reduced (control, 279 ± 41 s and PR^{Cre}, 121 ± 19 s; n ≥ 10, p = 3 × 10⁻³). In summary, targeted ablation of adult PR+ VMHvl neurons led to a significant diminution in female mating.

We assessed the ablation of PR+ VMHvl cells in these PR^{Cre} females. We observed that most (97% ± 1; n = 10 control and 16 PR^{Cre} females) PR+ VMHvl neurons were ablated upon injection of the taCasp3-encoding AAV into PR^{Cre} females (Figure 5G). Coinjection of this AAV and a constitutively expressed, EGFP-encoding AAV revealed spread to the adjacent arcuate nucleus, which contains PR+ neurons (Figure 2I–2L) and controls feeding and the estrous cycle (Atasoy et al., 2012; Simerly, 2002). Consistent with the lack of estrous cycle or body weight phenotypes in PR^{Cre} mice (see below and Figure S5), our injections spared most PR+ arcuate neurons in PR^{Cre} females (74% ± 12 of controls). There was no correlation in the extent of loss of PR+ arcuate neurons and reduced sexual receptivity ($R^2 = 5 \times 10^{-3}$, p = 0.8). Moreover, we found that PR^{Cre} females (n = 7) in whom the number of PR+ arcuate neurons was indistinguishable from controls also rejected males and displayed reduced sexual receptivity (rejections per assay: controls, 1 ± 1 and PR^{Cre} females, 35 ± 7, p ≤ 6 × 10⁻⁵, n ≥ 7; receptivity index: controls, 0.5 and PR^{Cre} females 0.2 ± 0.1, p ≤ 3 × 10⁻³, n ≥ 7). Thus, PR+ VMHvl neurons are required for normal female sexual behavior.

We tested the specificity of the behavioral deficit in PR^{Cre} females after the ablation of PR+ VMHvl neurons. Despite their reduced sexual receptivity, these mice sniffed and groomed males normally (Figures S5C and S5D) (groom duration: control, 2 ± 1 s and PR^{Cre}, 5 ± 1 s; n ≥ 10, p ≥ 0.3). There were no overt deficits in tests of anxiety, motivated behavior, motor coordination, and locomotor activity (Figures S5E–S5H). In contrast to the weight gain subsequent to a VMH lesion (Dhillon et al., 2006; Hetherington and Ranson, 1940; King, 2006; Majdic et al., 2002), PR^{Cre} females maintained body weight similar to controls upon ablation of PR+ VMHvl neurons (Figure S5I). Thus, we have partitioned the VMHvl to reveal that PR+ VMHvl neurons are required for normal levels of female sexual receptivity, but not for all social or other behaviors and physiology.

In separate studies, we ablated PR+ VMHvl neurons but left the ovaries intact in order to examine whether other female-typical behaviors were regulated by these neurons. This ablation did not disrupt the estrous cycle, as assayed by vaginal cytology (Figure S5J). To test for maternal behaviors, we obtained litters from PR^{Cre} and control females by cohousing them with WT males. Similar to control females, PR^{Cre} females displayed various elements of maternal care toward their litters, including pup retrieval and aggression toward unfamiliar intruders in their cage (Figures S5K–S5O). Therefore, our results show that ablation of PR+ VMHvl neurons reduced female sexual displays without overt disruption of other female-typical behaviors and physiology.

PR regulates female mating (Lydon et al., 1995), and our findings suggest that it functions in the VMHvl to do so, which is consistent with prior work (Mani et al., 1994a, 1994b; Ogawa et al., 1994; Pollio et al., 1993). Cckar is also required for female mating (Xu et al., 2012). Most Cckar+ VMHvl neurons are PR+ (Figures S2C–S2E), resulting in a near-complete loss of these

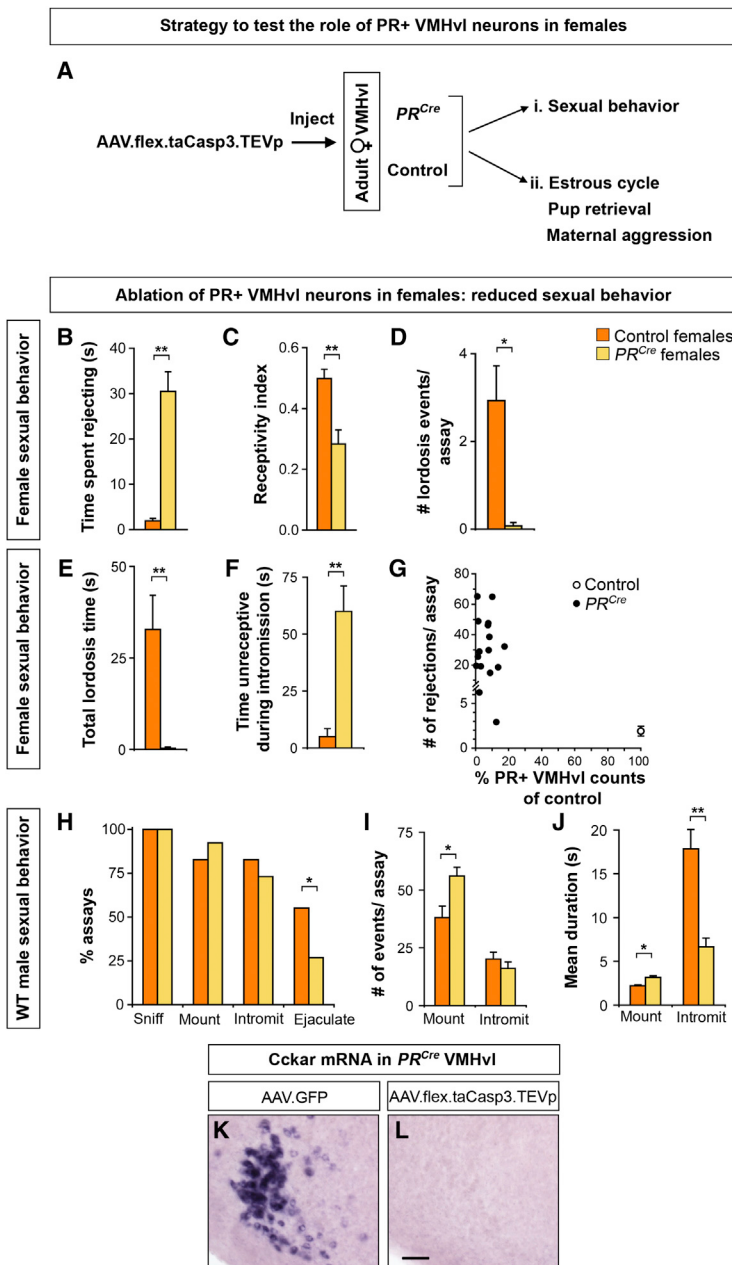


Figure 5. PR+ VMHvl Neurons Regulate Female Sexual Receptivity

(A) An experimental design to test the role of PR+ VMHvl neurons in female behaviors. Mating was tested with ovariectomized females primed to be in estrus. Other behaviors were tested with gonadally intact females.

(B–J) PR^{Cre} and control females were injected with AAV-flex-taCasp3-TEVp and tested for sexual behavior with WT males.

(B) PR^{Cre} females spend more time rejecting male mating attempts and walking away when the male approaches.

(C–E) PR^{Cre} females display a lower receptivity index (mounts leading to intromission divided by total mounts) and a reduced number and duration of lordosis events.

(F) PR^{Cre} females spend more time moving about and being unresponsive during intromission.

(G) Fewer than 20% of PR+ neurons remain in the VMHvl of PR^{Cre} females, who reject male mating attempts more than control females.

(H) Males sniff and initiate mating equally as often with PR^{Cre} and WT females but ejaculate in fewer assays with PR^{Cre} females.

(I) Males mount PR^{Cre} females more often but do so without a corresponding increase in intromission.

(J) Males mount PR^{Cre} females longer but intromit for a shorter duration.

(K and L) Ablation of PR+ VMHvl neurons in PR^{Cre} females results in a loss of Cckar expression.

Mean ± SEM; n ≥ 10 per experimental group (B–J); n = 3 (K and L).

*, p < 0.02; **, p < 0.005. The scale bar represents 50 μm.

Also see Figure S5, Table S3, and Movies S1, and S2.

cells upon ablation of PR+ VMHvl neurons (Figures 5K and 5L). It is possible that PR or Cckar act elsewhere to control female mating and that these genes only mark a pool of VMHvl neurons that control this behavior. We favor a more parsimonious model in which PR and Cckar function in the VMHvl to regulate female mating. In any event, our findings show that PR+ Cckar+ VMHvl neurons are essential for high WT levels of female sexual behavior.

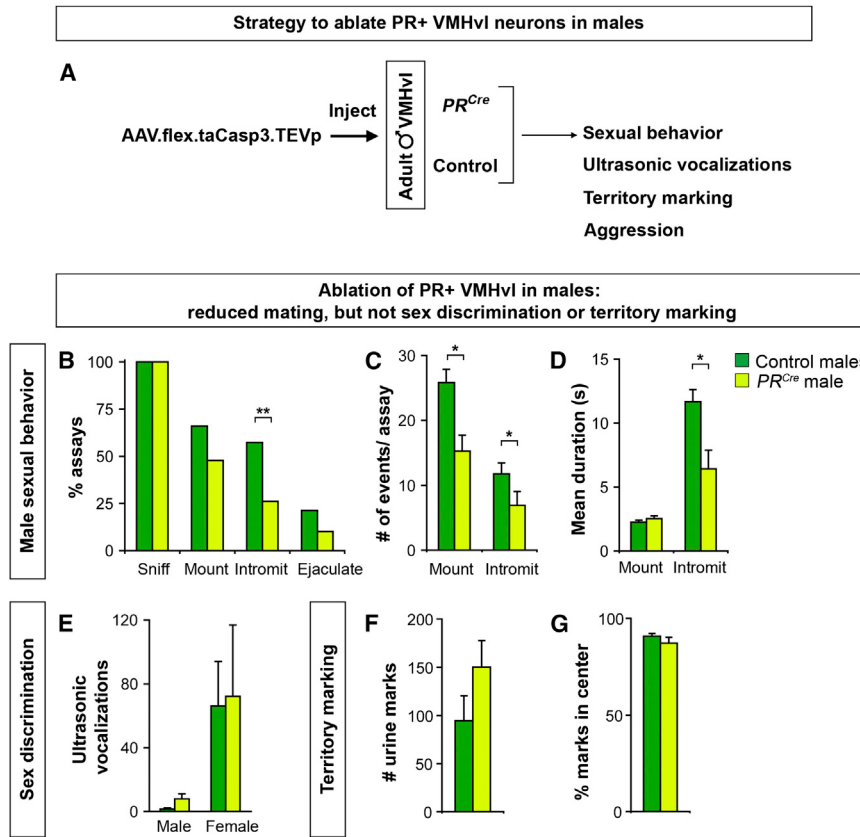
The Dimorphic PR+ VMHvl Cluster of Neurons Regulates Mating and Aggression in Males

The VMH has been implicated in regulating female mating and male fighting. PR+ neurons represent ~50% of VMHvl neurons,

and these neurons regulate female mating (Figure 5), but fighting could be controlled by PR+ or PR– VMH cells. We tested whether PR+ VMHvl neurons regulate male behaviors by ablating them with the taCasp3-encoding AAV (Figure 6A). PR^{Cre} and control males were allowed to recover for 4 weeks following viral delivery and were singly housed and tested for mating and fighting.

PR^{Cre} and control males initiated mounting intruder females in a similar manner, but PR^{Cre} males were less likely to intromit (Figures 6B and S6A). The reduced intromissions most likely resulted from the fewer mounts exhibited by PR^{Cre} males (Figure 6C). Even when these males intromitted, there was a decrease in the number and duration of intromissions (Figures 6D, 6E, and S6B). The decreased intromission count was significant (n ≥ 16 per cohort; p = 5 × 10⁻³)

even when normalized to the fewer mounts. Thus, ablation of male PR+ VMHvl neurons led to specific deficits in the consummatory elements of mating. This phenotype was not accompanied by deficits in preservatively appetitive behaviors, such as sniffing (Figures 6B and S6C–S6E), sex discrimination, or territory marking. There was no difference between PR^{Cre} and control males in sex discrimination, as shown by predominantly female-directed ultrasonic vocalization (Figure 6E) (Nyby et al., 1977). Both PR^{Cre} and control males also marked their territory equivalently (Figures 6F and 6G) (Desjardins et al., 1973; Kimura and Hagiwara, 1985). Altogether, this evidence suggests that PR+ VMHvl neurons are essential for the normal display of male sexual behavior.



We tested whether ablation of PR+ VMHvl neurons disrupted aggression toward a WT male intruder. *PR^{Cre}* males exhibited a >2-fold reduction in the probability of initiating aggression in comparison to controls (Figure 7A). Even when *PR^{Cre}* males fought, they attacked less often, for a shorter duration, and with a longer interval between attacks (Figures 7B–7D). Male fighting includes tail rattles and overt attacks, such as biting. Control and *PR^{Cre}* residents rattled their tails in a similar manner, but *PR^{Cre}* males bit intruders over 3-fold less (Figure 7E). Thus, ablation of PR+ VMHvl neurons significantly reduces male aggression.

We assessed the ablation of PR+ VMHvl neurons in males tested behaviorally. Most of these neurons (95% ± 1; n = 14 control and 35 *PR^{Cre}* males) were ablated in *PR^{Cre}* males (Figure 7F–7H), whereas PR+ arcuate neurons were largely spared (92% ± 12 of controls). There was no correlation in the extent of loss of PR+ neurons in the arcuate and the reduced mating or fighting (mating: $R^2 = 4 \times 10^{-4}$, p = 0.9; fighting: $R^2 = 2 \times 10^{-2}$, p = 0.7). *PR^{Cre}* males (n = 15) in whom the number of PR+ arcuate neurons was indistinguishable from controls also exhibited deficits in mating and fighting (percentage of males intromitting: controls, 67% and *PR^{Cre}*, 27%, n ≥ 15, p = 0.02; percentage of males attacking: controls, 75% and *PR^{Cre}*, 20%, n ≥ 15, p = 1 × 10⁻³). Altogether, our findings demonstrate that PR+ VMHvl neurons control the normal display of male mating and fighting.

We tested the specificity of the deficits in *PR^{Cre}* males following ablation of PR+ VMHvl neurons. Despite deficits in

Figure 6. PR+ VMHvl Neurons Regulate Male Sexual Behavior

(A) An experimental design to test the role of PR+ VMHvl neurons in male behaviors.

(B–G) *PR^{Cre}* and control males were injected with AAV-flex-taCasp3-TEVp and tested for mating, ultrasonic vocalizations toward male or female intruders, and territory marking.

(B) *PR^{Cre}* males intromit females in fewer assays.

(C and D) *PR^{Cre}* males mount and intromit females less often and have shorter bouts of intromission.

(E) Both *PR^{Cre}* and control males emit more vocalizations to females.

(F and G) There was no difference between *PR^{Cre}* and control males in the number and distribution of urine marks. % marks in center equals 100 × (the number urine marks not abutting cage perimeter divided by the number of all urine marks).

Mean ± SEM; n ≥ 24 per experimental group

(B–D, F, and G), n ≥ 5 per experimental group (E).

*, p < 0.008; **, p < 0.001.

Also see Figures S6 and S7.

mating and fighting, these males sniffed and groomed intruders in a WT manner (Figures 6B, 7A, S6C–S6E, S7A–S7C). *PR^{Cre}* males performed at WT levels in assays of anxiety, motivated behavior, motor coordination, and locomotor activity (Figures S7D–S7G). These males maintained normal body weight, and there was no change in the weight of

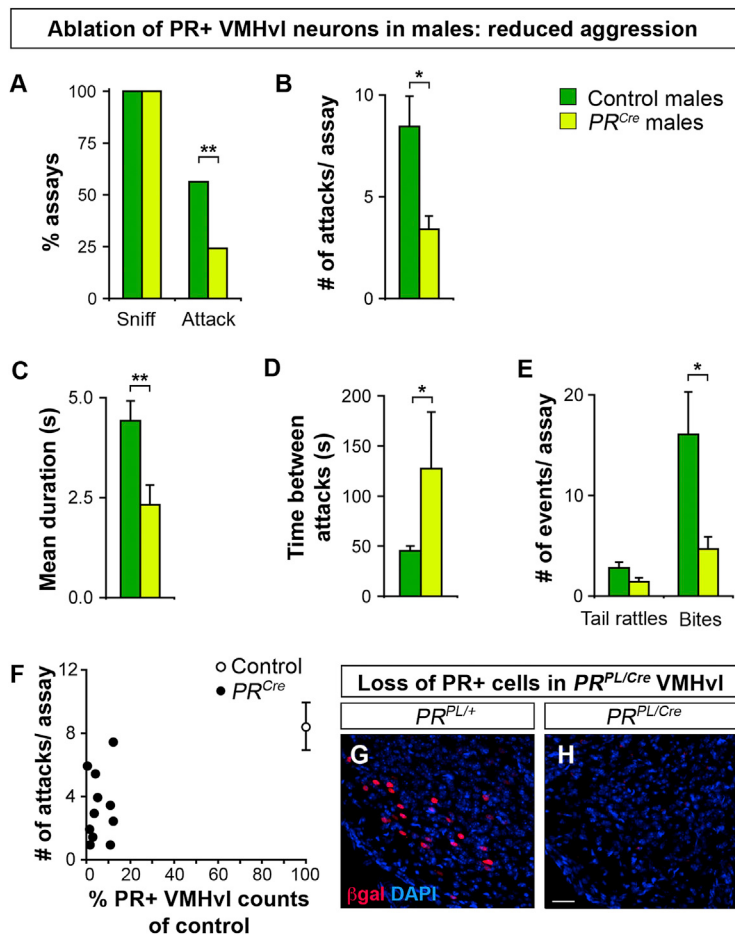
gonads and seminal vesicles and serum testosterone titers (Figures S7H–S7J). Thus, PR+ VMHvl neurons are specifically required in males for the high WT levels of mating and aggression.

DISCUSSION

We have identified a small, sexually dimorphic cluster of ~2,000 PR+ hypothalamic neurons that is essential for the normal display of sexual receptivity in females and sexual and aggressive behaviors in males. Our findings directly demonstrate that sexually dimorphic neurons in the brain influence dimorphic behaviors. Moreover, these PR+ neurons are functionally bivalent in that they regulate distinct dimorphic behaviors in the two sexes.

Control of Social Behaviors by the VMH

Experimental studies and clinical observations have long suggested that the VMH or adjacent hypothalamic regions regulate aggression and female mating (Bard, 1928; Blaustein, 2008; Clemente and Chase, 1973; Colpaert and Wiepkema, 1976; Grossman, 1972; Hess and Akert, 1955; Kow et al., 1985; Kruk et al., 1979; Lin et al., 2011; Olivier and Wiepkema, 1974; Pfaff and Sakuma, 1979a, 1979b; Reeves and Plum, 1969; Swaab, 2003; La Vaque and Rodgers, 1975; Wheatley, 1944). Despite intense scrutiny, the neurons that control these behaviors remained unidentified. In fact, whether separate or

**Figure 7. PR+ VMHvl Neurons Regulate Male Aggression**

(A–F) PR^{Cre} and control resident males were injected with AAV-flex-taCasp3-TEVp targeted to the VMHvl and tested for aggression toward a WT male intruder.

(A) All residents sniff intruders equivalently, but PR^{Cre} males attack less.

(B–D) When PR^{Cre} males fight, they attack less, for a shorter duration, and with longer intervals between attacks.

(E) PR^{Cre} males bite less often.

(F) Fewer than 20% of PR+ neurons remain in the VMHvl of PR^{Cre} males, who attack intruders less often. Mean \pm SEM; n = 24 per experimental group. *, p < 0.04; **, p ≤ 0.009.

(G and H) Ablation of PR+ VMHvl neurons in a PR^{PL/Cre} male injected with AAV-flex-taCasp3-TEVp. The scale bar represents 25 μ m.

Also see Figure S7.

Distributive Neural Control of Sexually Dimorphic Behaviors

It is curious that ablation of a highly restricted, molecularly defined set of neurons results in deficits in both male mating and fighting. These PR+ neurons may integrate social cues relevant to both behaviors, allowing males to mate or fight appropriately. Such dual control could also reflect further diversity within PR+ VMHvl neurons such that subsets of these neurons regulate one or the other behavior. In fact, in vivo recordings and c-Fos studies (Lin et al., 2011) reveal male VMHvl neurons that are activated during encounters with both sexes as well as neurons that appear responsive to either male or female encounters.

We find that different components of male behaviors require distinct neuronal populations. Males lacking PR+ VMHvl neurons have a male behavioral repertoire: they distinguish between the sexes with vocalizations (Stowers et al., 2002), attack males, and mate with females. Moreover, these males mark territory similarly to WT males, thereby providing an objective indicator that their internal representation of sexual identity is masculine. Nevertheless these males display specific deficits in mating and fighting, indicating that ablation of PR+ VMHvl neurons dissociates the repertoire of masculine behaviors. Such partial behavioral deficits could reflect compensatory mechanisms activated upon the loss of these neurons. However, acute inactivation of the VMH mimics the behavioral deficits we observed (Lin et al., 2011), suggesting a minimal role of compensatory mechanisms. Thus, male mating and fighting are encoded in a distributive or redundant manner in the brain. Similarly, ablation of these neurons reduced female sexual receptivity without overtly disrupting estrous cyclicity or maternal care behavior, indicating that these behaviors and physiology may also be controlled by distinct neuronal groups. Altogether, our findings show that sex-typical behaviors are represented distributively and that different neuronal populations in the underlying neural circuit control specific components of these behaviors. In fact, genes such as Cckar also control these behaviors in a modular manner; for instance, Cckar^{-/-} females show reduced sexual

overlapping neuronal groups control these innate behaviors was also unknown. Our studies reveal the molecular identity of the long sought-after neurons in or around the VMH that influence male fighting and female mating. Although other neighboring neurons may also influence these behaviors, we show that PR+ VMHvl neurons are required for the normal display of mating in females and fighting in males. These PR+ neurons also regulate male mating. Nontargeted inhibition of neurons in this region disrupts male fighting, but not male mating (Lin et al., 2011), suggesting partial inactivation or incomplete targeting of the neurons that regulate male mating. By contrast, our ablation of the PR+ VMHvl population revealed a role for these cells in male mating. Generalized arousal systems may feed into the VMH to enhance social interactions (Schober et al., 2011). We did not observe altered locomotor activity, sensorimotor coordination, or general social interactions in mice lacking PR+ VMHvl neurons, suggesting that these neurons are unlikely to exert a major influence on neural pathways that increase such arousal. In summary, we show that PR+ VMHvl neurons are required for the normal display of mating in both sexes and fighting in males. Given the conservation of genes and neuroanatomy across placental mammals, these VMHvl neurons may regulate mating and aggression in many mammals, including humans.

receptivity without alterations in other behaviors or physiology (Xu et al., 2012). Thus, modular control of sexually dimorphic behaviors across multiple levels, including genes and neurons, may be a general organizational principle of the underlying neural circuits.

Control of Sex-Typical Behaviors by Sexually Dimorphic VMHvl Neurons

Studies in diverse animals have defined the relevance of particular brain regions to sex-typical behaviors (Brenowitz, 1991; Cooke et al., 1998; Ferveur et al., 1995; Kelley, 1997; Konishi, 1989; Morris et al., 2004). However, within a brain region, only specific subsets of neurons are sexually dimorphic (Ng et al., 2009; De Vries and Panzica, 2006; Xu et al., 2012), and with rare exceptions in invertebrates (Kohatsu et al., 2011; von Philipsborn et al., 2011), the function of sexually dimorphic neurons is unknown. Ablation of the ~2,000 sexually dimorphic PR+ VMHvl neurons, a fraction of the ~10⁸ neurons in the mouse brain, results in specific deficits in complex social behaviors. Such specificity most likely results from the manipulation of a molecularly defined subset of neurons. Indeed, PR+ neurons represent only ~50% of VMHvl neurons that, in turn, represent a fraction of VMH neurons.

The mechanisms whereby sexually dimorphic neurons control dimorphic behaviors are poorly understood. It is possible that PR+ VMHvl neurons represent unrelated cell types in the two sexes, as evidenced by the sex differences in cell number and distribution, projection targets, and expression of Cckar. This is unlikely, given that PR+ VMHvl neurons also share many features, including location, projection targets, gene expression (PR, ER α), and developmental lineage (Grgurevic et al., 2012). Thus, it appears that a common pool of PR+ VMHvl neurons is present in both sexes, but their sex differences may allow them to transform synaptic inputs in a sex-specific manner or to relay male- or female-specific input in order to drive a sexually dimorphic behavioral output.

Most behaviors are common to both sexes, suggesting that each sex possesses the motor pathways to display dimorphic behaviors of the opposite sex. Most sex differences in the brain represent quantitative and not all-or-none cellular or molecular sex differences. It is unknown whether these shared, but dimorphic, neurons regulate sex-typical behaviors in both sexes. Alternatively, such neurons may regulate a dimorphic output in one sex, and, in the other sex, they may be functionally vestigial, subserve a nondimorphic function, or suppress a function of the opposite sex (De Vries and Boyle, 1998). We show that PR+ VMHvl neurons are functionally bivalent in the sense that they control sex-typical behaviors in both males and females. This dual function may prove adaptive if such neurons can generate a dimorphic behavior of the opposite sex in the appropriate context; in addition, bivalence may permit facile interchange of sex-typical behaviors between the sexes during speciation. Such flexibility may underlie the rapid evolution of sexually dimorphic traits (Darwin, 1871), including behaviors such as the allocation of parental care and social dominance hierarchies. Given such evolutionary considerations, it remains to be seen whether all sexually dimorphic neuronal populations control sex-typical behaviors in both sexes.

EXPERIMENTAL PROCEDURES

Viruses

AAV-flex-taCasp3-TEVp

The plasmid encoding AAV-flex-taCasp3-TEVp (Figure S4A) was generated with routine subcloning. High-titer virus of serotype 2/1 (3×10^{12} IU/mL) was generated from the plasmid at the University of North Carolina Vector Core.

Lenti-lxlap

The plasmid encoding this VSVG pseudotyped lentivirus was generated with standard subcloning (Figure S3G). High-titer virus (~10⁸ IU/mL) was generated with standard protocols (Barde et al., 2001).

Stereotaxic Surgery

The virus was stereotactically delivered under anesthesia to the VMHvl (coordinates: rostrocaudal, -1.48 mm; mediolateral, ±0.78 mm; depth, 5.8 mm; also see the Extended Experimental Procedures) (Paxinos and Franklin, 2003). Injections of taCasp3-encoding AAV were spiked (9:1) with constitutive EGFP-encoding AAV in order to verify the accuracy of the injection placement in control and *PR*^{Cre} mice.

Behavior

Testing was performed as described previously (Juntti et al., 2010; Wu et al., 2009; Xu et al., 2012) (also see the Extended Experimental Procedures). To test for sexual receptivity, we castrated females and, subsequent to estrus induction with estrogen and progesterone, inserted them singly into the home cage of a sexually experienced WT male. Lordosis was defined as the female holding still with a dorsiflexed neck while being intromitted. Each experimental cohort included a set of control and *PR*^{Cre} mice.

Details regarding animals, histology, data analyses, and the procedures described above can be found in the Extended Experimental Procedures. All animal studies were in accordance with Institutional Animal Care and Use Committee protocols at the University of California, San Francisco.

SUPPLEMENTAL INFORMATION

Supplemental Information includes Extended Experimental Procedures, seven figures, three tables, and two movies and can be found with this article online at <http://dx.doi.org/10.1016/j.cell.2013.04.017>.

ACKNOWLEDGMENTS

We thank C. Saper for sharing reagents; A. Lasek and U. Heberlein for a practical on stereotaxis; R. Axel for discussions; R. Axel, T. Clandinin, H. Ingraham, S. Lomvardas, C. Saper, and members of the Shah lab for comments on the manuscript; and N. Agarwal, A. Wang, and M. Borius for technical support. This work was supported by a Genentech Graduate Fellowship (C.F.Y.); a National Science Foundation Graduate Fellowship (S.A.J.); the National Institutes of Health (NIH) grant F31NS078959 (E.K.U.); the Brain and Behavior Research Foundation Program in Biomedical Breakthrough Research, Ellison Medical Foundation; and NIH grants R01NS049488 and DP1MH099900 (N.M.S.).

Received: December 5, 2012

Revised: February 11, 2013

Accepted: April 5, 2013

Published: May 9, 2013

REFERENCES

- Allen, E. (1922). The oestrous cycle in the mouse. Am. J. Anat. 30, 297–371.
- Atasoy, D., Aponte, Y., Su, H.H., and Sternson, S.M. (2008). A FLEX switch targets Channelrhodopsin-2 to multiple cell types for imaging and long-range circuit mapping. J. Neurosci. 28, 7025–7030.

- Atasoy, D., Betley, J.N., Su, H.H., and Sternson, S.M. (2012). Deconstruction of a neural circuit for hunger. *Nature* 488, 172–177.
- Bard, P. (1928). A diencephalic mechanism for the expression of rage with special reference to the sympathetic nervous system. *Am. J. Physiol.* 84, 490–515.
- Barde, I., Salmon, P., and Trono, D. (2001). Production and Titration of Lentiviral Vectors. Current Protocols in Neuroscience (Hoboken, NJ: John Wiley & Sons, Inc.).
- Becker, J.B. (1999). Gender differences in dopaminergic function in striatum and nucleus accumbens. *Pharmacol. Biochem. Behav.* 64, 803–812.
- Blaustein, J.D. (2008). Neuroendocrine regulation of feminine sexual behavior: lessons from rodent models and thoughts about humans. *Annu. Rev. Psychol.* 59, 93–118.
- Blaustein, J.D., and Feder, H.H. (1979). Cytoplasmic progestin-receptors in guinea pig brain: characteristics and relationship to the induction of sexual behavior. *Brain Res.* 169, 481–497.
- Blaustein, J.D., Ryer, H.I., and Feder, H.H. (1980). A sex difference in the progestin receptor system of guinea pig brain. *Neuroendocrinology* 31, 403–409.
- Brenowitz, E.A. (1991). Altered perception of species-specific song by female birds after lesions of a forebrain nucleus. *Science* 251, 303–305.
- Brown, T.J., Yu, J., Gagnon, M., Sharma, M., and MacLusky, N.J. (1996). Sex differences in estrogen receptor and progestin receptor induction in the guinea pig hypothalamus and preoptic area. *Brain Res.* 725, 37–48.
- Bunting, M., Bernstein, K.E., Greer, J.M., Copech, M.R., and Thomas, K.R. (1999). Targeting genes for self-excision in the germ line. *Genes Dev.* 13, 1524–1528.
- Chappell, P.E., Lydon, J.P., Conneely, O.M., O'Malley, B.W., and Levine, J.E. (1997). Endocrine defects in mice carrying a null mutation for the progesterone receptor gene. *Endocrinology* 138, 4147–4152.
- Clemente, C.D., and Chase, M.H. (1973). Neurological substrates of aggressive behavior. *Annu. Rev. Physiol.* 35, 329–356.
- Cohen, R.S., and Pfaff, D.W. (1992). Ventromedial hypothalamic neurons in the mediation of long-lasting effects of estrogen on lordosis behavior. *Prog. Neurobiol.* 38, 423–453.
- Colpaert, F.C., and Wiepkema, P.R. (1976). Effects of ventromedial hypothalamic lesions on spontaneous intraspecies aggression in male rats. *Behav. Biol.* 16, 117–125.
- Cooke, B., Hegstrom, C.D., Villeneuve, L.S., and Breedlove, S.M. (1998). Sexual differentiation of the vertebrate brain: principles and mechanisms. *Front. Neuroendocrinol.* 19, 323–362.
- Darwin, C. (1871). The Descent of Man, and Selection in Relation to Sex (Princeton, NJ: Princeton University Press).
- De Vries, G.J. (1990). Sex differences in neurotransmitter systems. *J. Neuroendocrinol.* 2, 1–13.
- De Vries, G.J., and Boyle, P.A. (1998). Double duty for sex differences in the brain. *Behav. Brain Res.* 92, 205–213.
- De Vries, G.J., and Panzica, G.C. (2006). Sexual differentiation of central vasopressin and vasotocin systems in vertebrates: different mechanisms, similar endpoints. *Neuroscience* 138, 947–955.
- Desjardins, C., Maruniak, J.A., and Bronson, F.H. (1973). Social rank in house mice: differentiation revealed by ultraviolet visualization of urinary marking patterns. *Science* 182, 939–941.
- Dewing, P., Shi, T., Horvath, S., and Vilain, E. (2003). Sexually dimorphic gene expression in mouse brain precedes gonadal differentiation. *Brain Res. Mol. Brain Res.* 118, 82–90.
- Dhillon, H., Zigman, J.M., Ye, C., Lee, C.E., McGovern, R.A., Tang, V., Kenny, C.D., Christiansen, L.M., White, R.D., Edelstein, E.A., et al. (2006). Leptin directly activates SF1 neurons in the VMH, and this action by leptin is required for normal body-weight homeostasis. *Neuron* 49, 191–203.
- Dugger, B.N., Morris, J.A., Jordan, C.L., and Breedlove, S.M. (2007). Androgen receptors are required for full masculinization of the ventromedial hypothalamus (VMH) in rats. *Horm. Behav.* 51, 195–201.
- Ferveur, J.F., Störtkuhl, K.F., Stocker, R.F., and Greenspan, R.J. (1995). Genetic feminization of brain structures and changed sexual orientation in male Drosophila. *Science* 267, 902–905.
- Flanagan-Cato, L.M. (2011). Sex differences in the neural circuit that mediates female sexual receptivity. *Front. Neuroendocrinol.* 32, 124–136.
- Flanagan-Cato, L.M., Lee, B.J., and Calizo, L.H. (2006). Co-localization of midbrain projections, progestin receptors, and mating-induced fos in the hypothalamic ventromedial nucleus of the female rat. *Horm. Behav.* 50, 52–60.
- Gagnidze, K., Pfaff, D.W., and Mong, J.A. (2010). Gene expression in neuroendocrine cells during the critical period for sexual differentiation of the brain. *Prog. Brain Res.* 186, 97–111.
- Gorski, R.A., Harlan, R.E., Jacobson, C.D., Shryne, J.E., and Southam, A.M. (1980). Evidence for the existence of a sexually dimorphic nucleus in the preoptic area of the rat. *J. Comp. Neurol.* 193, 529–539.
- Goy, R.W., and Phoenix, C.H. (1963). Hypothalamic regulation of female sexual behaviour; establishment of behavioural oestrus in spayed guinea-pigs following hypothalamic lesions. *J. Reprod. Fertil.* 5, 23–40.
- Gray, D.C., Mahrus, S., and Wells, J.A. (2010). Activation of specific apoptotic caspases with an engineered small-molecule-activated protease. *Cell* 142, 637–646.
- Grgurevic, N., Büdefeld, T., Spanic, T., Tobet, S.A., and Majdic, G. (2012). Evidence that sex chromosome genes affect sexual differentiation of female sexual behavior. *Horm. Behav.* 61, 719–724.
- Grossman, S.P. (1972). Aggression, avoidance, and reaction to novel environments in female rats with ventromedial hypothalamic lesions. *J. Comp. Physiol. Psychol.* 78, 274–283.
- Harvey, W. (1651). Exercitationes de generatione animalium. In The Works of William Harvey, R. Willis, tr. (Miami, FL: HardPress Publishing), pp. 186–187.
- Hess, W.R., and Akert, K. (1955). Experimental data on role of hypothalamus in mechanism of emotional behavior. *AMA Arch. Neurol. Psychiatry* 73, 127–129.
- Hetherington, A.W., and Ranson, S.W. (1940). Hypothalamic lesions and adiposity in the rat. *Anat. Rec.* 78, 149–172.
- Jazin, E., and Cahill, L. (2010). Sex differences in molecular neuroscience: from fruit flies to humans. *Nat. Rev. Neurosci.* 11, 9–17.
- Jiang, X., and Wang, X. (2004). Cytochrome C-mediated apoptosis. *Annu. Rev. Biochem.* 73, 87–106.
- Juntti, S.A., Tollkühn, J., Wu, M.V., Fraser, E.J., Soderborg, T., Tan, S., Honda, S.-I., Harada, N., and Shah, N.M. (2010). The androgen receptor governs the execution, but not programming, of male sexual and territorial behaviors. *Neuron* 66, 260–272.
- Kelley, D.B. (1997). Generating sexually differentiated songs. *Curr. Opin. Neurobiol.* 7, 839–843.
- Kimura, T., and Hagiwara, Y. (1985). Regulation of urine marking in male and female mice: effects of sex steroids. *Horm. Behav.* 19, 64–70.
- King, B.M. (2006). The rise, fall, and resurrection of the ventromedial hypothalamus in the regulation of feeding behavior and body weight. *Physiol. Behav.* 87, 221–244.
- Kohatsu, S., Koganezawa, M., and Yamamoto, D. (2011). Female contact activates male-specific interneurons that trigger stereotypic courtship behavior in Drosophila. *Neuron* 69, 498–508.
- Kollack-Walker, S., and Newman, S.W. (1995). Mating and agonistic behavior produce different patterns of Fos immunolabeling in the male Syrian hamster brain. *Neuroscience* 66, 721–736.
- Konishi, M. (1989). Birdsong for neurobiologists. *Neuron* 3, 541–549.
- Kow, L.M., Harlan, R.E., Shivers, B.D., and Pfaff, D.W. (1985). Inhibition of the lordosis reflex in rats by intrahypothalamic infusion of neural excitatory agents: evidence that the hypothalamus contains separate inhibitory and facilitatory elements. *Brain Res.* 341, 26–34.
- Krieger, M.S., Conrad, L.C., and Pfaff, D.W. (1979). An autoradiographic study of the efferent connections of the ventromedial nucleus of the hypothalamus. *J. Comp. Neurol.* 183, 785–815.

- Kruk, M.R., van der Poel, A.M., and de Vos-Frerichs, T.P. (1979). The induction of aggressive behaviour by electrical stimulation in the hypothalamus of male rats. *Behaviour* 70, 292–322.
- Kudwa, A.E., Harada, N., Honda, S.-I., and Rissman, E.F. (2009). Regulation of progestin receptors in medial amygdala: estradiol, phytoestrogens and sex. *Physiol. Behav.* 97, 146–150.
- Kurrasch, D.M., Cheung, C.C., Lee, F.Y., Tran, P.V., Hata, K., and Ingraham, H.A. (2007). The neonatal ventromedial hypothalamus transcriptome reveals novel markers with spatially distinct patterning. *J. Neurosci.* 27, 13624–13634.
- La Vaque, T.J., and Rodgers, C.H. (1975). Recovery of mating behavior in the female rat following VMH lesions. *Physiol. Behav.* 14, 59–63.
- Leal, S., Andrade, J.P., Paula-Barbosa, M.M., and Madeira, M.D. (1998). Arcuate nucleus of the hypothalamus: effects of age and sex. *J. Comp. Neurol.* 401, 65–88.
- Leedy, M.G., and Hart, B.L. (1985). Female and male sexual responses in female cats with ventromedial hypothalamic lesions. *Behav. Neurosci.* 99, 936–941.
- Levine, J.E., Chappell, P.E., Schneider, J.S., Sleiter, N.C., and Szabo, M. (2001). Progesterone receptors as neuroendocrine integrators. *Front. Neuroendocrinol.* 22, 69–106.
- Lin, D., Boyle, M.P., Dollar, P., Lee, H., Lein, E.S., Perona, P., and Anderson, D.J. (2011). Functional identification of an aggression locus in the mouse hypothalamus. *Nature* 470, 221–226.
- Lydon, J.P., DeMayo, F.J., Funk, C.R., Mani, S.K., Hughes, A.R., Montgomery, C.A., Jr., Shyamala, G., Conneely, O.M., and O'Malley, B.W. (1995). Mice lacking progesterone receptor exhibit pleiotropic reproductive abnormalities. *Genes Dev.* 9, 2266–2278.
- Majdic, G., Young, M., Gomez-Sanchez, E., Anderson, P., Szczepaniak, L.S., Dobbins, R.L., McGarry, J.D., and Parker, K.L. (2002). Knockout mice lacking steroidogenic factor 1 are a novel genetic model of hypothalamic obesity. *Endocrinology* 143, 607–614.
- Mani, S.K., Allen, J.M., Clark, J.H., Blaustein, J.D., and O'Malley, B.W. (1994a). Convergent pathways for steroid hormone- and neurotransmitter-induced rat sexual behavior. *Science* 265, 1246–1249.
- Mani, S.K., Blaustein, J.D., Allen, J.M., Law, S.W., O'Malley, B.W., and Clark, J.H. (1994b). Inhibition of rat sexual behavior by antisense oligonucleotides to the progesterone receptor. *Endocrinology* 135, 1409–1414.
- Mani, S.K., Blaustein, J.D., and O'Malley, B.W. (1997). Progesterone receptor function from a behavioral perspective. *Horm. Behav.* 31, 244–255.
- Mathews, D., and Edwards, D.A. (1977a). Involvement of the ventromedial and anterior hypothalamic nuclei in the hormonal induction of receptivity in the female rat. *Physiol. Behav.* 19, 319–326.
- Mathews, D., and Edwards, D.A. (1977b). The ventromedial nucleus of the hypothalamus and the hormonal arousal of sexual behaviors in the female rat. *Horm. Behav.* 8, 40–51.
- Matsumoto, A., and Arai, Y. (1983). Sex difference in volume of the ventromedial nucleus of the hypothalamus in the rat. *Endocrinol. Jpn.* 30, 277–280.
- Matsumoto, A., and Arai, Y. (1986). Male-female difference in synaptic organization of the ventromedial nucleus of the hypothalamus in the rat. *Neuroendocrinology* 42, 232–236.
- Maxwell, I.H., Maxwell, F., and Glode, L.M. (1986). Regulated expression of a diphtheria toxin A-chain gene transfected into human cells: possible strategy for inducing cancer cell suicide. *Cancer Res.* 46, 4660–4664.
- McCarthy, M.M., and Arnold, A.P. (2011). Reframing sexual differentiation of the brain. *Nat. Neurosci.* 14, 677–683.
- McGill, T.E. (1962). Sexual behavior in three inbred strains of mice. *Behavior* 19, 341–350.
- Morris, J.A., Jordan, C.L., and Breedlove, S.M. (2004). Sexual differentiation of the vertebrate nervous system. *Nat. Neurosci.* 7, 1034–1039.
- Morris, J.A., Jordan, C.L., and Breedlove, S.M. (2008). Sexual dimorphism in neuronal number of the posterodorsal medial amygdala is independent of circulating androgens and regional volume in adult rats. *J. Comp. Neurol.* 506, 851–859.
- Musatov, S., Chen, W., Pfaff, D.W., Kaplitt, M.G., and Ogawa, S. (2006). RNAi-mediated silencing of estrogen receptor alpha in the ventromedial nucleus of hypothalamus abolishes female sexual behaviors. *Proc. Natl. Acad. Sci. USA* 103, 10456–10460.
- Musatov, S., Chen, W., Pfaff, D.W., Mobbs, C.V., Yang, X.-J., Clegg, D.J., Kaplitt, M.G., and Ogawa, S. (2007). Silencing of estrogen receptor alpha in the ventromedial nucleus of hypothalamus leads to metabolic syndrome. *Proc. Natl. Acad. Sci. USA* 104, 2501–2506.
- Ng, L., Bernard, A., Lau, C., Overly, C.C., Dong, H.-W., Kuan, C., Pathak, S., Sunkin, S.M., Dang, C., Bohland, J.W., et al. (2009). An anatomic gene expression atlas of the adult mouse brain. *Nat. Neurosci.* 12, 356–362.
- Nyby, J., Wysocki, C.J., Whitney, G., and Dizinno, G. (1977). Pheromonal regulation of male mouse ultrasonic courtship (*Mus musculus*). *Anim. Behav.* 25, 333–341.
- Ogawa, S., Olazábal, U.E., Parhar, I.S., and Pfaff, D.W. (1994). Effects of intra-hypothalamic administration of antisense DNA for progesterone receptor mRNA on reproductive behavior and progesterone receptor immunoreactivity in female rat. *J. Neurosci.* 14, 1766–1774.
- Olivier, B., and Wiepkema, P.R. (1974). Behaviour changes in mice following electrolytic lesions in the median hypothalamus. *Brain Res.* 65, 521–524.
- Olster, D.H., and Blaustein, J.D. (1990). Immunocytochemical colocalization of progestin receptors and beta-endorphin or enkephalin in the hypothalamus of female guinea pigs. *J. Neurobiol.* 21, 768–780.
- Patisaul, H.B., Fortino, A.E., and Polston, E.K. (2008). Sex differences in serotonergic but not gamma-aminobutyric acidergic (GABA) projections to the rat ventromedial nucleus of the hypothalamus. *Endocrinology* 149, 397–408.
- Paxinos, G., and Franklin, K.B.J. (2003). *The Mouse Brain in Stereotaxic Coordinates: Compact, Second Edition* (Waltham, MA: Academic Press).
- Pfaff, D.W., and Sakuma, Y. (1979a). Deficit in the lordosis reflex of female rats caused by lesions in the ventromedial nucleus of the hypothalamus. *J. Physiol.* 288, 203–210.
- Pfaff, D.W., and Sakuma, Y. (1979b). Facilitation of the lordosis reflex of female rats from the ventromedial nucleus of the hypothalamus. *J. Physiol.* 288, 189–202.
- Phelps, S.M., Lydon, J.P., O'malley, B.W., and Crews, D. (1998). Regulation of male sexual behavior by progesterone receptor, sexual experience, and androgen. *Horm. Behav.* 34, 294–302.
- Pollio, G., Xue, P., Zanisi, M., Nicolin, A., and Maggi, A. (1993). Antisense oligonucleotide blocks progesterone-induced lordosis behavior in ovariectomized rats. *Brain Res. Mol. Brain Res.* 19, 135–139.
- Power, R.F., Mani, S.K., Codina, J., Conneely, O.M., and O'Malley, B.W. (1991). Dopaminergic and ligand-independent activation of steroid hormone receptors. *Science* 254, 1636–1639.
- Quadros, P.S., Pfau, J.L., Goldstein, A.Y.N., De Vries, G.J., and Wagner, C.K. (2002). Sex differences in progesterone receptor expression: a potential mechanism for estradiol-mediated sexual differentiation. *Endocrinology* 143, 3727–3739.
- Quadros, P.S., Schlueter, L.J., and Wagner, C.K. (2008). Distribution of progesterone receptor immunoreactivity in the midbrain and hindbrain of postnatal rats. *Dev. Neurobiol.* 68, 1378–1390.
- Reeves, A.G., and Plum, F. (1969). Hyperphagia, rage, and dementia accompanying a ventromedial hypothalamic neoplasm. *Arch. Neurol.* 20, 616–624.
- Ricciardi, K.H., and Blaustein, J.D. (1994). Projections from ventrolateral hypothalamic neurons containing progestin receptor- and substance P-immunoreactivity to specific forebrain and midbrain areas in female guinea pigs. *J. Neuroendocrinol.* 6, 135–144.
- Robarts, D.W., and Baum, M.J. (2007). Ventromedial hypothalamic nucleus lesions disrupt olfactory mate recognition and receptivity in female ferrets. *Horm. Behav.* 51, 104–113.

- Rubin, B.S., and Barfield, R.J. (1983). Induction of estrous behavior in ovariectomized rats by sequential replacement of estrogen and progesterone to the ventromedial hypothalamus. *Neuroendocrinology* 37, 218–224.
- Sakuma, Y., and Pfaff, D.W. (1979). Facilitation of female reproductive behavior from mesensephalic central gray in the rat. *Am. J. Physiol.* 237, R278–R284.
- Saper, C.B., Swanson, L.W., and Cowan, W.M. (1976). The efferent connections of the ventromedial nucleus of the hypothalamus of the rat. *J. Comp. Neurol.* 169, 409–442.
- Schneider, J.S., Burgess, C., Sleiter, N.C., DonCarlos, L.L., Lydon, J.P., O'Malley, B., and Levine, J.E. (2005). Enhanced sexual behaviors and androgen receptor immunoreactivity in the male progesterone receptor knockout mouse. *Endocrinology* 146, 4340–4348.
- Schneider, J.S., Burgess, C., Horton, T.H., and Levine, J.E. (2009). Effects of progesterone on male-mediated infant-directed aggression. *Behav. Brain Res.* 199, 340–344.
- Schober, J., Weil, Z., and Pfaff, D. (2011). How generalized CNS arousal strengthens sexual arousal (and vice versa). *Horm. Behav.* 59, 689–695.
- Shah, N.M., Pisapia, D.J., Maniatis, S., Mendelsohn, M.M., Nemes, A., and Axel, R. (2004). Visualizing sexual dimorphism in the brain. *Neuron* 43, 313–319.
- Simerly, R.B. (2002). Wired for reproduction: organization and development of sexually dimorphic circuits in the mammalian forebrain. *Annu. Rev. Neurosci.* 25, 507–536.
- Smith, R.L., Geller, A.I., Escudero, K.W., and Wilcox, C.L. (1995). Long-term expression in sensory neurons in tissue culture from herpes simplex virus type 1 (HSV-1) promoters in an HSV-1-derived vector. *J. Virol.* 69, 4593–4599.
- Stowers, L., Holy, T.E., Meister, M., Dulac, C., and Koentges, G. (2002). Loss of sex discrimination and male-male aggression in mice deficient for TRP2. *Science* 295, 1493–1500.
- Swaab, D. (2003). The ventromedial nucleus (VMN; nucleus of Cajal). In *The Human Hypothalamus: Basic and Clinical Aspects Part I: Nuclei of the Human Hypothalamus* (Amsterdam: Elsevier), pp. 239–242.
- Tsutsui, K. (2012). Neurosteroid biosynthesis and action during cerebellar development. *Cerebellum* 11, 414–415.
- Veening, J.G., Coolen, L.M., de Jong, T.R., Joosten, H.W., de Boer, S.F., Koolhaas, J.M., and Olivier, B. (2005). Do similar neural systems subserve aggressive and sexual behaviour in male rats? Insights from c-Fos and pharmacological studies. *Eur. J. Pharmacol.* 526, 226–239.
- von Philipsborn, A.C., Liu, T., Yu, J.Y., Masser, C., Bidaye, S.S., and Dickson, B.J. (2011). Neuronal control of *Drosophila* courtship song. *Neuron* 69, 509–522.
- Wheatley, M.D. (1944). The hypothalamus and affective behavior in cats: a study of the effects of experimental lesions, with anatomic correlations. *Arch Neuropsych* 52, 296–316.
- Witt, D.M., Young, L.J., and Crews, D. (1995). Progesterone modulation of androgen-dependent sexual behavior in male rats. *Physiol. Behav.* 57, 307–313.
- Wu, M.V., Manoli, D.S., Fraser, E.J., Coats, J.K., Tollkuhn, J., Honda, S.-I., Harada, N., and Shah, N.M. (2009). Estrogen masculinizes neural pathways and sex-specific behaviors. *Cell* 139, 61–72.
- Xu, X., Coats, J.K., Yang, C.F., Wang, A., Ahmed, O.M., Alvarado, M., Izumi, T., and Shah, N.M. (2012). Modular genetic control of sexually dimorphic behaviors. *Cell* 148, 596–607.
- Yang, X., Schadt, E.E., Wang, S., Wang, H., Arnold, A.P., Ingram-Drake, L., Drake, T.A., and Lusis, A.J. (2006). Tissue-specific expression and regulation of sexually dimorphic genes in mice. *Genome Res.* 16, 995–1004.

Supplemental Information

EXTENDED EXPERIMENTAL PROCEDURES

Animals

Adult mice 10–24 weeks of age were used in all studies. Mice were housed in an UCSF barrier facility with a 12:12 hr light:dark cycle, and food and water were available ad libitum. *PR*^{Cre/Cre} or *PR*^{Cre/+} mice and their control WT siblings were used to trace projections of PR+ VMHvl neurons. *PR*^{Cre/Cre} or *PR*^{Cre/PL} mice and their control (WT or *PR*^{PL}) same-sex siblings were used for behavioral studies. Animals were group-housed by sex after weaning at 3 weeks of age.

Generation of *PR*^{PL} and *PR*^{Cre} Knockin Mice

Genomic clones containing the last exon of *PR* were obtained by screening a 129/SvJ lambda phage library from Stratagene. An ~8.3 kb *BamHI* genomic clone containing the last two exons of *PR* was used to design the targeting vector. An *Ascl* restriction site was inserted 3 bp 3' of the stop codon of the *PR* gene using site-directed mutagenesis (Stratagene). This mutagenized targeting vector has 4.2 kb and 4.1 kb of homology 5' and 3' of the *Ascl* restriction site, respectively. To generate the *PR*^{PL} mice, we utilized the self-excising neomycin cassette, pACN, which was subcloned 3' of IRES-PLAP-IRES-nuclear LacZ (Bunting et al., 1999; Shah et al., 2004). This IRES-PLAP-IRES-nuclear LacZ-ACN cassette was inserted into the targeting vector as an *Ascl* fragment. The PR-IRES-PLAP-IRES-nuclear LacZ-ACN targeting vector was electroporated into a 129/SvEv mouse embryonic stem (ES) cell line. We obtained a targeting frequency of 44% for homologous recombinants, which were detected using PCR for the 3' arm for the targeting vector. We used a primer (F3) that was complementary to the ACN cassette and an external primer (R2) that was complementary to genomic sequence located 3' of the 3' homology arm of the targeting vector (see Table S3 for all primer sequences used in our study). A subset of positive clones was tested by PCR for homologous targeting of the 5' arm using an external primer (F1) and a primer unique to the modified allele (R1). ES clones harboring the homologously recombined *PR* allele were injected into blastocysts to obtain chimeric mice which were crossed to C57Bl/6J females to obtain germline transmission. Chimeric mice that transmitted the *PR*^{PL} allele were obtained from one positive clone. ACN contains a *neomycin*^R gene that is self-excised upon passage through the male germline, and F1 progeny obtained by crossing the chimeric males to C57Bl/6J females had deleted ACN as determined by PCR using primers F2 and R2 (Figure 1B). The resulting progeny (backcrossed > 3 generations in C57Bl/6J) were used for experimental analysis. A similar strategy was used to generate mice bearing the *PR*^{Cre} allele. We flanked with FRT sites the DNA fragment encoding RNA PolII promoter-Neo^R-pA of pACN to generate the pFNF selection cassette. This FNF cassette was subcloned 3' of IRES-Cre to generate the plasmid pCre-FNF. The IRES-Cre-FNF cassette was inserted into the targeting vector as an *Ascl* fragment into the *Ascl* site engineered 3 bp 3' of the *PR* stop codon. The targeting vector was electroporated into a 129/SvEv mouse ES cell line, and we obtained a targeting frequency of 14% for homologous recombinants. To detect positive clones, we performed PCR for the 3' arm for the targeting vector. We used a primer (F3) that was complementary to the FNF cassette and an external primer (R2) as above. A subset of positive clones was tested by PCR for homologous targeting of the 5' arm using an external primer (F1) and a primer unique to the modified allele (R1). ES clones harboring the homologously recombined *PR*^{Cre} allele were injected into blastocysts to obtain chimeric mice that were crossed to C57Bl/6J females to obtain germline transmission. Chimeric mice that transmitted the *PR*^{Cre} allele were obtained from one positive clone. We bred the F1 progeny of these chimeras to mice expressing Flpe recombinase ubiquitously (Rodríguez et al., 2000). Deletion of the FNF cassette was verified by PCR and sequencing of the PCR product. The resulting progeny (backcrossed > 3 generations in C57Bl/6J) were behaviorally and physiologically WT and used for experimental analysis. Both the *PR*^{PL} and the *PR*^{Cre} lines were maintained either by breeding with C57Bl/6J mice or breedings between heterozygotes. Experimental animals were largely derived from such breedings and occasionally from breedings between a mouse homozygote and a mouse heterozygote for these alleles.

Viruses

AAV-flex-taCasp3-TEVp

The *taCasp3-T2A-TEVp* transgene was generated by overlapping PCR of plasmids harboring taCasp3 and TEVp (Gray et al., 2010). This transgene was inserted in reverse orientation into the plasmid pAAV-EF1a-DIO-hChr2(H134R)-EYFP-WPRE-pA such that it replaced hChr2(H134R)-EYFP (Zhang et al., 2006). This yielded the plasmid encoding AAV-flex-taCasp3-TEVp (Figure S4A).

Lenti-*Ixlplap*

The pHIV-CSCG vector (Miyoshi et al., 1998) served as the backbone in the generation of the plasmid encoding this virus. A *histone 2B:EGFP* fusion transgene was flanked by loxP sites such that the 5' loxP site intervened between the ATG and the rest of the transgene, and multiple stop codons in all reading frames were inserted 5' of the 3' loxP site. This histone 2B:EGFP encoding translational stop cassette (*Ixl*) was inserted 3' of the Ubiquitin ligase C promoter in the modified pHIV-CSCG. A PLAP-encoding transgene lacking the first ATG was subcloned 3' of the stop cassette to generate the plasmid pLenti-*Ixlplap*.

Stereotaxic Surgery

A mouse was placed in a stereotaxic frame (Kopf Instruments) under anesthesia, the skull was exposed with a midline scalp incision, and the stereotaxic frame was aligned at bregma using visual landmarks. The drill (drill bit #85; ~279 μm diameter) on the stereotaxic frame was placed over the skull at coordinates corresponding to the VMHvl (rostrocaudal, -1.48 mm; mediolateral, ± 0.78 mm), and a hole was drilled through the skull bone to expose the brain. A 33 gauge steel needle loaded with virus was aligned at bregma

(including in the z axis) and slowly inserted through the hole at 1 mm/min until it penetrated to a depth of 5.8 mm. Virus was delivered (1 μ l of AAV; 0.8 μ l of lentivirus) at 100 nL/min with a Hamilton syringe by hand or using a syringe pump (Harvard Apparatus). Injections of taCasp3-encoding AAV were spiked (9:1) with constitutive EGFP-encoding AAV of the same serotype to verify accuracy of the injection placement in control and PR^{Cre} mice. The needle was left for an additional 10 min to allow diffusion of the virus, and it was withdrawn at 1 mm/min. Mice were allowed to recover individually over a heating pad in fresh cages and when mobile returned to their home cage.

qRT-PCR

We collected 200 μ m thick coronal slices from acutely dissected 10-12 week old brains of C57Bl/6J mice using a vibrating microtome (Leica) into a dish containing ice-cold d-PBS (free of Ca^{2+} and Mg^{2+}). The basal forebrain, AVPV/POA, BNST, VMHvl, arcuate, cingulate cortex, dentate gyrus, and MeA were dissected from these slices using a stereomicroscope and landmarks from the mouse brain atlas (Paxinos and Franklin, 2003), and the tissue fragments were immediately frozen on dry ice. Total RNA was extracted with Trizol, treated with DNase I and subjected to first strand cDNA synthesis using random hexamers as well as oligo-dT primed reactions (SuperScript III, Invitrogen). qPCR was performed using the primers for PR mRNA (Table S3) on an Eppendorf Mastercycler EP using 2XSYBR master mix (Fermentas). A separate real time PCR reaction (primers listed in Table S3) to detect expression of the ubiquitous ribosomal message Rpl32 was used to permit normalization of PR expression levels in each of the brain regions.

Histology

Sexually naive, group-housed, age-matched mice were used in all histological studies to quantify sex differences in PR expression or projections of PR+ neurons. PLAP and β -gal histochemistry was performed as described previously on vibratome-collected coronal sections of 80 μ m thicknesses (Shah et al., 2004; Wu et al., 2009). PLAP-labeled projections were imaged in brightfield illumination and analyzed using NIH ImageJ software. For each of the projection targets (AVPV, POA, and PAG) of the PR+ VMHvl neurons, we quantitated the projections in the entire region of interest using previously described protocols (Wu et al., 2009; Xu et al., 2012).

Immunolabeling was performed using 65 μ m thick vibratome brain sections using previously published protocols (Shah et al., 2004; Wu et al., 2009). The primary antisera used are: rabbit anti- β -gal (ICL, 1:5000), chicken anti- β -gal (Abcam, 1:6000), mouse anti-NeuN (Chemicon, 1:300), rabbit anti-ER α (Millipore, 1:10000), rabbit anti-GFP (Invitrogen, 1:2000). The fluorophore conjugated secondary antisera are: Cy3 donkey anti-rabbit, Cy3 donkey anti-chicken (Jackson ImmunoResearch, 1:800), Cy5 donkey anti-mouse (Jackson ImmunoResearch, 1:300), and AlexaFluor 488 donkey anti-rabbit (Invitrogen, 1:300). To quantitate sex differences in PR expression, we enumerated β -gal+ cells from $PR^{PL/PL}$ mice on both sides of the brain (left and right) individually for each region of interest and obtained the mean for each animal. These cells were imaged with confocal microscopy (Zeiss) as described earlier, using methods validated with unbiased stereology (Wu et al., 2009). An identical approach was used to enumerate β -gal+ cells in the VMH subsequent to delivery of the taCasp3-encoding AAV. To enumerate β -gal+ cells along the entire rostrocaudal extent of the hypothalamus in these studies, we imaged every third section in this region (starting from the AVPV to the mamillary bodies) and quantitated the cells as described earlier, using methods validated with unbiased stereology (Wu et al., 2009).

Cckar, Cre, and PR probes for *in situ* hybridization (ISH) were generated from subcloned RT-PCR products (primers listed in Table S3). The ISH was performed as described previously (Xu et al., 2012). Briefly, mice were perfused with 4% paraformaldehyde (PFA), and the brains were dissected, post-fixed, and sectioned at 100 μ m with a vibrating microtome (Leica). Sections were treated with proteinase K (10 μ g/mL, Roche) and fixed at room temperature. Sections were then acetylated and equilibrated to hybridization solution for 2-5 hr at 65°C, followed by incubation at 65°C overnight in hybridization buffer containing 0.5 μ g/mL digoxigenin-labeled RNA probe. The sections were then washed in high stringency buffers and incubated overnight at 4°C in buffer containing alkaline phosphatase-conjugated sheep anti-digoxigenin antibody (Roche, 1:2000). The sections were then incubated for 4-6 hr at 37°C in staining solution containing nitro blue tetrazolium and 5-bromo-4-chloro-3-indolyl-phosphate (NBT and BCIP, respectively; Roche). Finally, sections were washed, post-fixed, and mounted on glass slides. mRNA expression was quantified as described previously (Xu et al., 2012).

For dual colorimetric *in situ* hybridization and fluorescent immunolabeling, adult brains were fresh frozen in embedding medium (M1 Embedding Matrix, Thermo Scientific) and cryosectioned at 16 μ m on to glass slides (Superfrost, Fisher Scientific). Sections were fixed in 4% PFA and then acetylated as described previously (Juntti et al., 2010). After permeabilization with 1% Triton X-100, sections were incubated with prehybridization solution in a humidifying chamber for 2-4 hr at room temperature. Sections were hybridized with digoxigenin-UTP-labeled Cckar riboprobe (0.3 μ g /ml) overnight at 65°C. After washes, brain sections were incubated with sheep anti-digoxigenin conjugated to alkaline phosphatase (Roche, 1:5,000) and chicken anti- β -gal (Abcam, 1:3,000) in 5% heat inactivated serum from sheep and donkey overnight at 4°C. The sections were washed and stained using a colorimetric reaction with NBT/BCIP (Roche) at 37°C overnight. The reaction was stopped with PBS containing 1 mM EDTA, and the sections were washed and incubated with a secondary antibody, donkey anti-chicken Cy3 antibody (Jackson ImmunoResearch, 1:800), and DAPI for 2 hr at room temperature. After washes and a 10 min post-fix in 4% PFA, slides were coverslipped with Aquamount mounting medium (Polysciences). We imaged these sections on an upright microscope (Zeiss) using a 20X objective, switching between brightfield illumination (Cckar) and epifluorescence (β -gal). These images were overlaid in Adobe Photoshop and enumerated for the region of interest (VMHvl). Detailed protocols are available upon request.

NeuroTrace 640/660 (Invitrogen, 1:200) was used per instructions from the manufacturer in sections immunolabeled for β -gal. To quantify nuclear and soma size of PR+ VMHvl neurons, β -gal and NeuN immunolabeled sections were imaged with a confocal microscope using a 63X objective lens. The center 3 optical slices for each z-stack were flattened (maximal projection) in ImageJ. The nuclear and soma profiles were outlined and measured in ImageJ.

Behavior and Physiology

All behavioral testing was initiated \geq 1 hr after onset of the dark cycle, and recorded and analyzed as described previously (Juntti et al., 2010; Wu et al., 2009; Xu et al., 2012). Mice were rested for \geq 2 days between behavioral tests, and residents were always exposed to a novel intruder. For tests of sexual receptivity, females were rested for 7–10 days after an assay to allow hormone levels to subside to baseline levels prior to estrus induction for the next assay.

For male mice, singly housed residents were tested two times each for sexual behavior for 30 min with a WT female intruder hormonally primed to be in estrus. These residents were then tested 2 times each for aggression with a WT group-housed male intruder for 15 min. Performance in urine marking was tested once for 60 min in a fresh cage following social experience. Males were tested for ultrasonic vocalizations once each for 3 min to a WT male and female intruder introduced separately into the cage. Following all behavioral testing, the males were sacrificed and blood was collected to determine serum hormone levels as described previously (Juntti et al., 2010; Wu et al., 2009; Xu et al., 2012).

To test females in assays of sexual receptivity, the ovaries were removed, and the mice were allowed to recover from surgery for 4 weeks. Prior to behavioral testing, the females were hormonally primed to be in estrus using previously published protocols (Ogawa et al., 2000; Ring, 1944; Xu et al., 2012). Briefly, we administered subcutaneously 17 β -estradiol benzoate on day –2 (10 μ g in 100 μ l sesame oil), day –1 (5 μ g in 50 μ l sesame oil), and progesterone (50 μ g in 50 μ l sesame oil) on the day of testing. The females were tested with resident males 4–6 hr after receiving progesterone for 30 min each in three assays.

For the rotarod test, we followed standard procedures described previously (Jones and Roberts, 1968; Juntti et al., 2010; Xu et al., 2012). In brief, the mice were tested on an accelerated rotarod set-up (Ugo Basile) for 5 min each. We monitored the amount of time each mouse could successfully remain on the rotarod. For the cookie finding test, we followed a previously described protocol (Xu et al., 2012). Briefly, mice were food deprived overnight and then placed into a fresh cage containing a cookie buried under the bedding. Their behavior was recorded for 3 min following which the assay was terminated. Each mouse was tested twice in this cookie finding assay, and performance was assessed by the average of these two tests. For the elevated plus maze test, mice were placed in the center of an elevated maze facing the open arm at the start of the assay (Walf and Frye, 2007). Time spent in the closed or open arms during a 5 min interval was recorded.

Pup retrieval and maternal aggression were tested in females impregnated by a WT male that were singly housed 3–5 days prior to parturition. At 2, 4, and 6 days after parturition, the dam was removed briefly from the cage, and 4 pups were scattered across the cage floor away from the nest. The dam was returned to the cage, and her ability to retrieve these pups to the nest was tested for 10 min. To test for maternal aggression, pups of postnatal age 8, 10, and 12 days were removed, and a group-housed adult WT male intruder was inserted into the cage for 15 min. The pups were returned to the mother at the end of each assay.

For assessing any change in body weight subsequent to ablation of PR+ VMHvl neurons, the mice were weighed immediately prior to stereotaxic injection of the taCasp3-encoding virus. The mice were weighed at the time of sacrifice (\sim 10 weeks) and analysis of histology through the hypothalamus.

Daily vaginal smears were obtained from group-housed females for 2 weeks, and the cytological characteristics of the smear were examined with brightfield optics as described previously (Xu et al., 2012). An experimenter blind to the genotypes independently scored the stage of the estrous cycle.

Hormone Assays

Hormone titers were assayed with kits from Cayman Chemicals (estradiol, progesterone) and DRG International (testosterone) according to the manufacturer's protocols. Trunk blood was collected at the time of sacrifice 2–3 hr after the onset of the dark cycle.

Data Analysis

Behavioral and histological studies were performed and analyzed while blinded to the relevant variables, including sex, genotype, virus injected, and hormone treatment. For analysis of noncategorical parameters of mating, aggression, and maternal care, we only included data from the animals that performed the behavior. Linear regression analysis was performed using MATLAB. We used Fisher's exact test to analyze categorical data. For all other comparisons, we first analyzed the data distribution with the Lillefors' goodness-of-fit test of normality. Data sets not violating this test of normality were analyzed with Student's t test; otherwise we used the nonparametric Wilcoxon rank sum test. We always processed in parallel \geq 1 mouse/sex for quantitating sex differences in PR+ neurons and \geq 1 mouse/genotype (control and PR^{Cre}) for analyzing ablations.

SUPPLEMENTAL REFERENCES

- Jones, B.J., and Roberts, D.J. (1968). The quantitative measurement of motor incoordination in naive mice using an accelerating rotarod. *J. Pharm. Pharmacol.* 20, 302–304.

- Miyoshi, H., Blömer, U., Takahashi, M., Gage, F.H., and Verma, I.M. (1998). Development of a self-inactivating lentivirus vector. *J. Virol.* 72, 8150–8157.
- Ogawa, S., Chester, A.E., Hewitt, S.C., Walker, V.R., Gustafsson, J.A., Smithies, O., Korach, K.S., and Pfaff, D.W. (2000). Abolition of male sexual behaviors in mice lacking estrogen receptors alpha and beta (alpha beta ERKO). *Proc. Natl. Acad. Sci. USA* 97, 14737–14741.
- Ring, J.R. (1944). The estrogen-progesterone induction of sexual receptivity in the spayed female mouse. *Endocrinology* 34, 269–275.
- Rodríguez, C.I., Buchholz, F., Galloway, J., Sequerra, R., Kasper, J., Ayala, R., Stewart, A.F., and Dymecki, S.M. (2000). High-efficiency deleter mice show that FLPe is an alternative to Cre-loxP. *Nat. Genet.* 25, 139–140.
- Walf, A.A., and Frye, C.A. (2007). The use of the elevated plus maze as an assay of anxiety-related behavior in rodents. *Nat. Protoc.* 2, 322–328.
- Zhang, F., Wang, L.-P., Boyden, E.S., and Deisseroth, K. (2006). Channelrhodopsin-2 and optical control of excitable cells. *Nat. Methods* 3, 785–792.

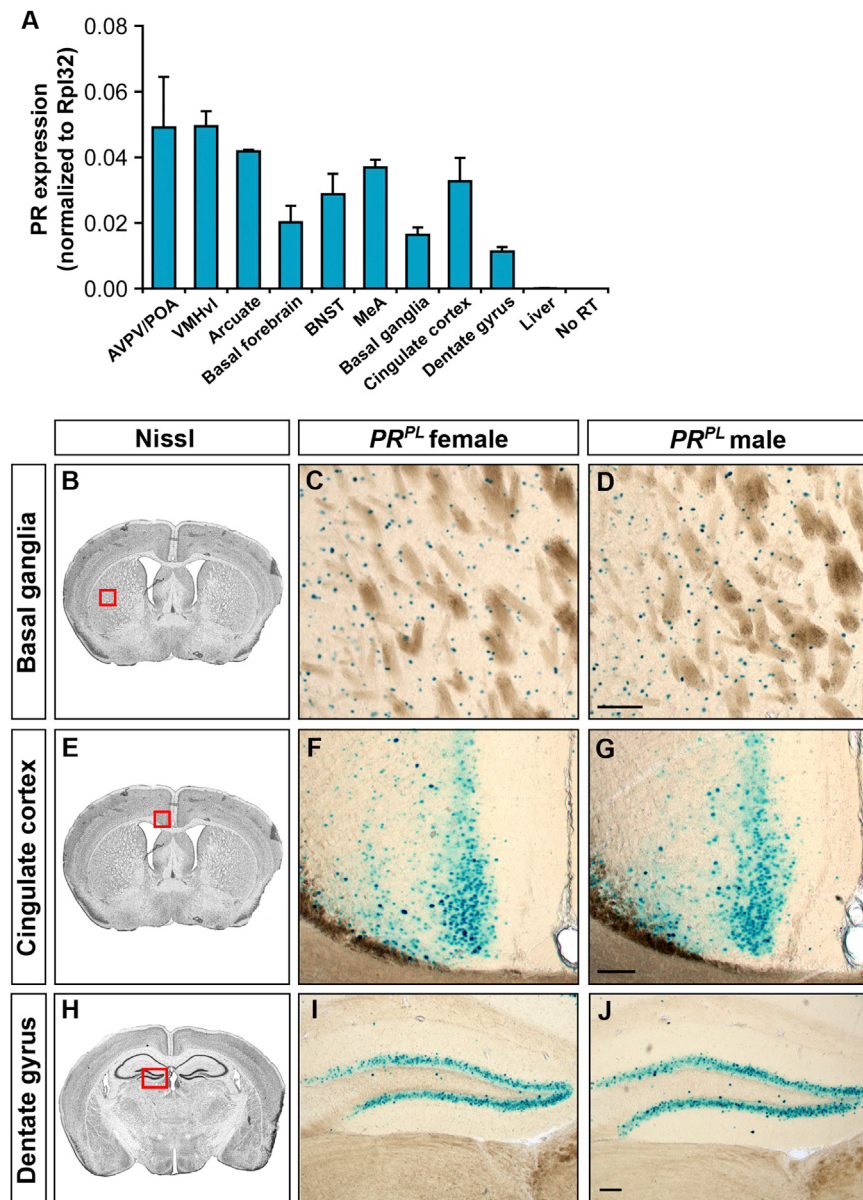


Figure S1. PR Expression in the WT and PR^{PL} Mouse Brain, Related to Figure 1

(A) Detection of PR by qRT-PCR in microdissected AVPV/POA, VMHvl, arcuate, basal forebrain, BNST, MeA, basal ganglia, cingulate cortex, and dentate gyrus, but not the liver of adult WT C57Bl/6J mice. The data presented is normalized to the expression of *Rpl32*, a housekeeping gene. Mean \pm SEM; n = 3. (B–J) PR is expressed in the basal ganglia, cingulate cortex, and dentate gyrus as visualized by β -gal activity in $PR^{PL/PL}$ female and male mice. Boxed area in Nissl-stained section indicates the region shown in the panels to the right. n \geq 3/sex. Scale bar equals 100 μ m.

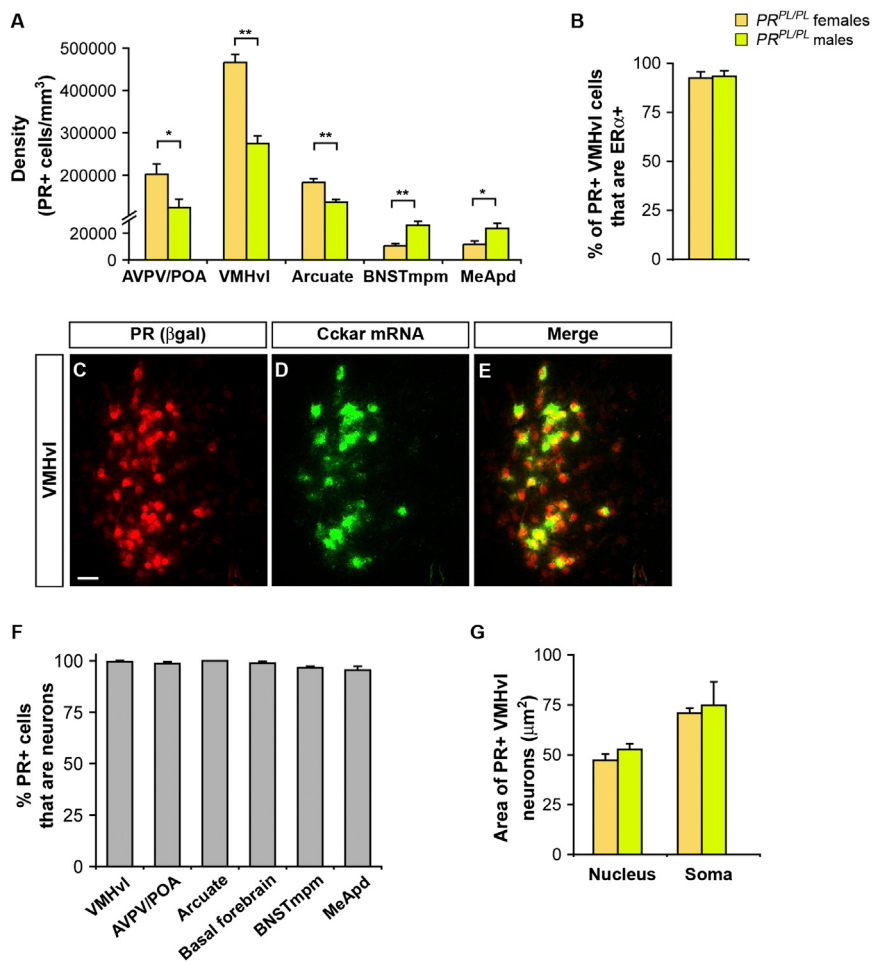


Figure S2. Characterization of Sexually Dimorphic PR Expression in PR^{PL} Mice, Related to Figure 2

(A) Sex differences in density of β -gal+ (PR^+) cells in adult $PR^{PL/PL}$ mice.

(B) A majority of PR^+ cells express $ER\alpha$, and there is no sex difference in co-labeling.

(C–E) Co-labeling VMHvl neurons for PR (anti- β -gal) and Cckar (mRNA) in $PR^{PL/PL}$ mice. The vast majority (~96%) of Cckar+ cells is PR^+ , whereas ~67% of PR^+ cells are Cckar+. Scale bar equals 25 μm .

(F) The vast majority of β -gal+ (PR^+) cells in various regions in PR^{PL} mice are neurons, as evidenced by co-labeling with NeuroTrace (fluorescent Nissl) in the arcuate and NeuN for the remaining regions.

(G) No sex difference in nuclear or soma size of PR^+ VMHvl cells in PR^{PL} mice. (>200 cells analyzed for each region).

Mean \pm SEM; n = 4/sex (A), n = 3 (B–G); *, p < 0.04, **, p < 0.008.

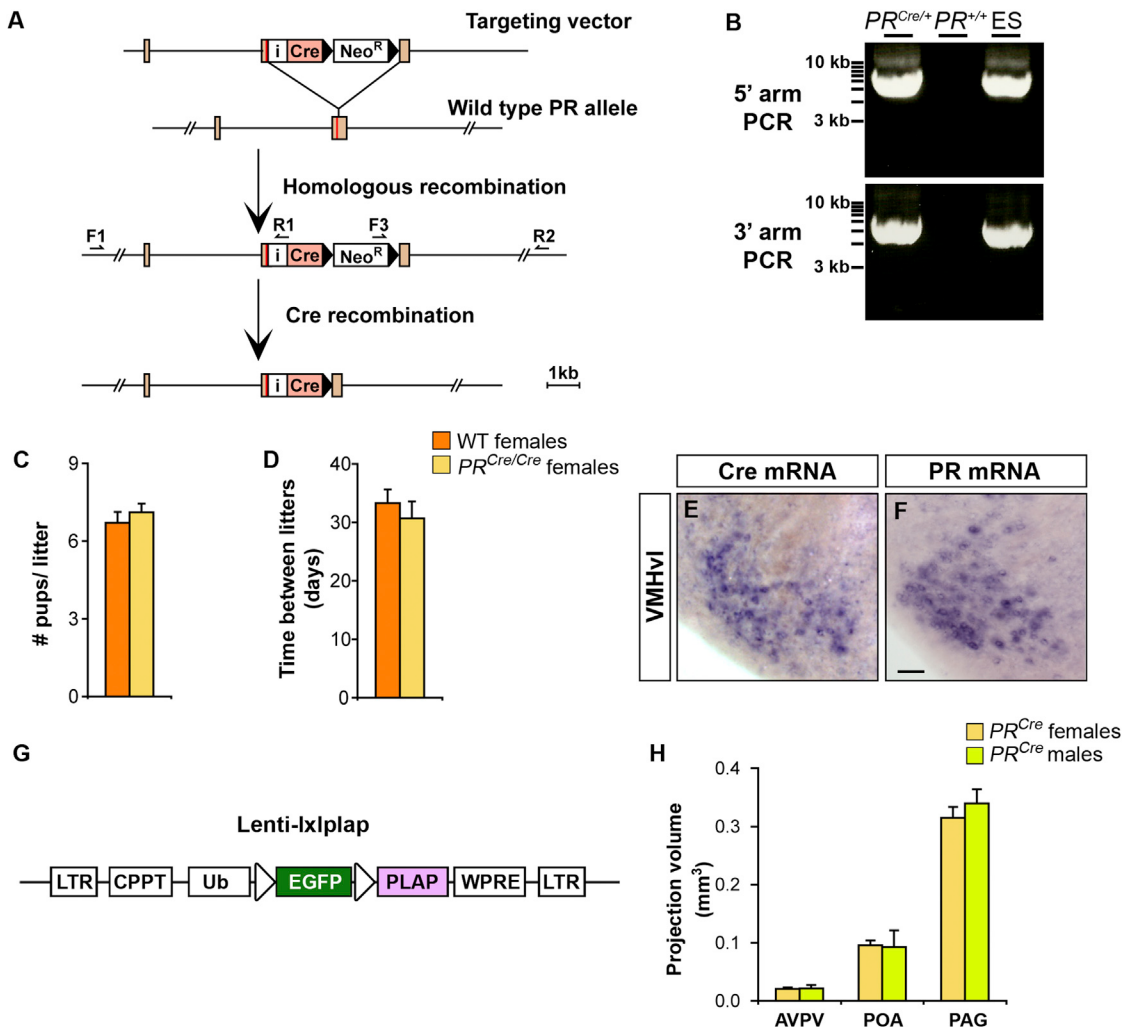


Figure S3. Mapping Projections of PR+ VMHvl Neurons in *PR*^{Cre} Knockin Mice, Related to Figure 3

(A) Schematic of the *PR* locus with the *IRES-Cre* transgene inserted 3' to the stop codon of the last exon. Primers used to detect integration of the 5' arm (F1, R1) and the 3' arm (F3, R2) only detect homologously recombined insertion events into the genome. Primer sequences listed in Table S3.

(B) PCR genotyping of *PR*^{Cre} allele. PCR primers are shown in (A). The FRT-flanked neomycin selection cassette was excised in vivo by crossing F1 progeny of *PR*^{Cre} chimeras bearing the targeted allele to mice expressing Flpe recombinase systemically (Rodríguez et al., 2000). Excision of the neomycin selection cassette leaves a single FRT site immediately 3' of *Cre*. We verified this excision event using primers (not shown) to amplify the 3' arm and sequencing through the remaining FRT site.

(C and D) No difference between WT and *PR*^{Cre/Cre} females in litter size and frequency. Mean ± SEM; n ≥ 12/genotype. Note that data from WT females shown here are from the same mice shown in Figures 1C and 1D.

(E and F) *Cre* expression mirrors that of PR in the VMHvl of adult *PR*^{Cre/+} mice in adjacent sections. n = 3. Scale bar equals 25 μm.

(G) DNA construct used to generate the Lenti-Ixlplap virus. The transgene is flanked by long terminal repeats (LTRs). A central polyA signal tract (CPPT) resides 5' of a Ubiquitin ligase C promoter (Ub), followed by a loxP-flanked histone 2B:EGFP. 3' of the 3' loxP site is the DNA encoding PLAP followed by a woodchuck post-transcriptional regulatory element (WPRE).

(H) No sex difference in the volume of PR+ VMHvl projections in the AVPV, POA, and PAG. The dense distribution of PLAP-labeled projections is only observed in the AVPV of females, but sparsely labeled fibers occupy a similar volume in the male AVPV. Mean ± SEM; n = 3/sex.

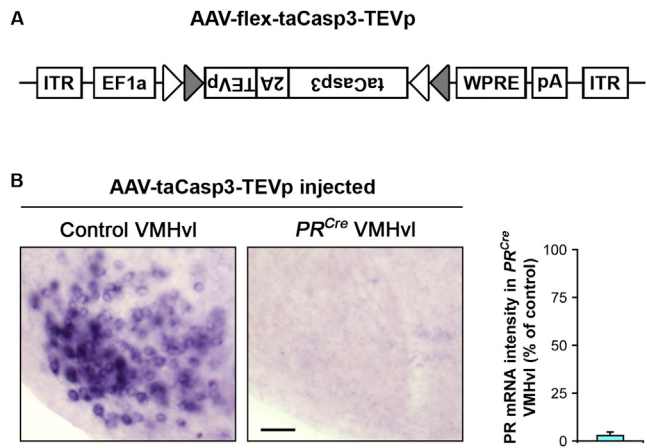


Figure S4. Ablation of PR+ VMHvl Cells in PR^{Cre} Mice with AAV-flex-taCasp3-TEVp, Related to Figure 4

(A) The DNA construct encoding AAV-flex-taCasp3-TEVp contains inverted terminal repeats (ITRs) flanking the transgene inserted into the viral genome. The transgene consists of an EF1a promoter 5' to an inverted taCasp3-T2A-TEVp sequence that is flanked by heterotypic loxP (open triangles) and lox2722 (closed triangles) sites. 3' of this transgene is a WPRE sequence and an hGH polyA signal sequence (pA).

(B) The vast majority of PR mRNA⁺ cells is lost upon caspase-mediated ablation of PR+ VMHvl neurons in $PR^{Cre/+}$ and $PR^{Cre/PL}$ male and female mice. Scale bar = 50 μ m. Mean \pm SEM; n = 5.

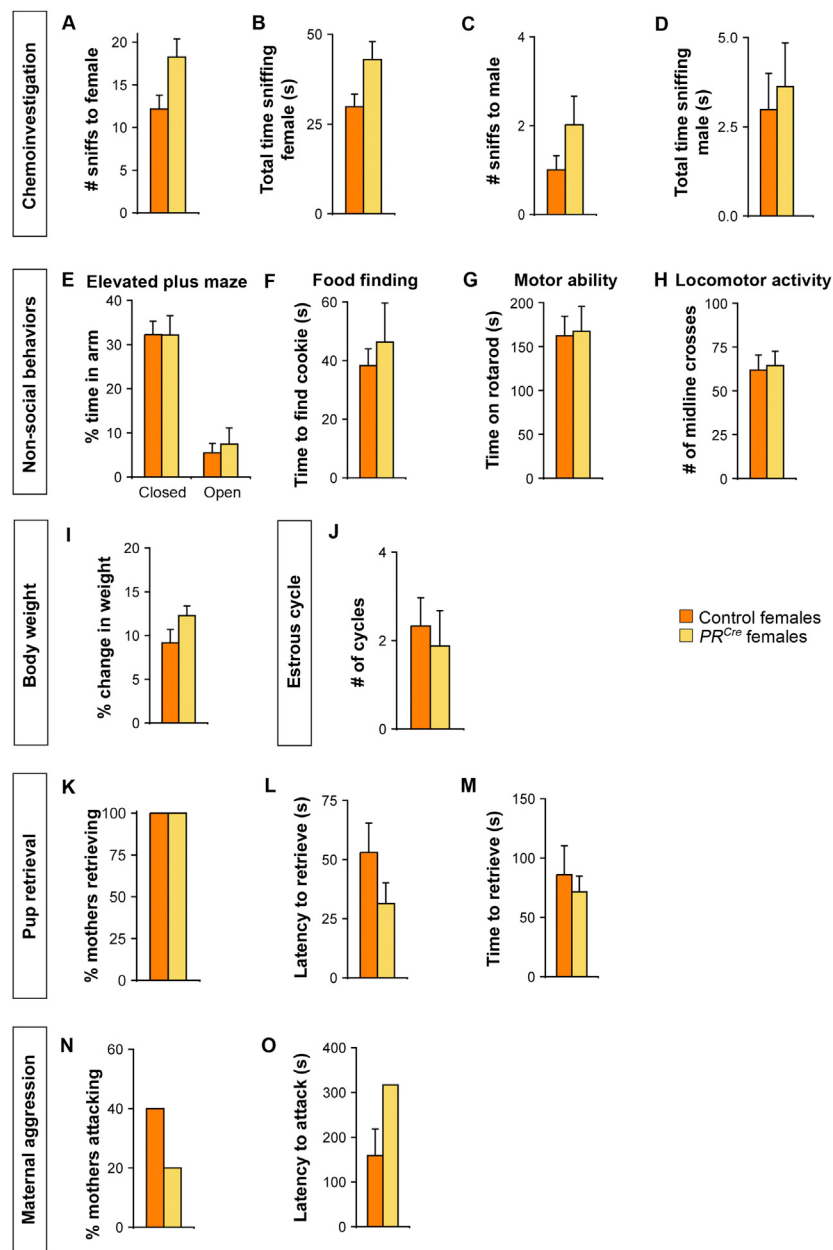


Figure S5. Females Lacking $PR+$ VMHvl Neurons Do Not Display Pervasive Deficits in Physiology or Behavior, Related to Figure 5

Adult PR^{Cre} and control females were injected with AAV-flex-taCasp3-TEVp targeted to the VMHvl and tested in different assays.

(A and B) WT males sniffed PR^{Cre} and control females equivalently. n ≥ 10/experimental group.

(C and D) No difference between PR^{Cre} and control females in sniffing WT males during assays of female sexual behavior. n ≥ 10/experimental group.

(E–H) No difference between PR^{Cre} and control females in tests of anxiety (E), motivation to find food (F), motor coordination and fatigue in the rotarod test (G), and general locomotor activity (H). n = 8/experimental group.

(I) No difference between PR^{Cre} and control females in percent change in body weight 10 weeks following viral injection. n ≥ 10/experimental group.

(J) No significant difference between PR^{Cre} and control females in the frequency of estrous cycles in 2 weeks. n ≥ 8/experimental group.

(K–O) The marked diminution in sexual receptivity subsequent to ablation of $PR+$ VMHvl neurons corresponded with fewer PR^{Cre} females delivering litters. Nevertheless in PR^{Cre} females bearing litters, there was no statistical difference between PR^{Cre} and control females in retrieving their pups (K–M) or attacking unfamiliar intruders in their cage (N, O). Only females who displayed pup retrieval or maternal aggression were included in the analysis of behavioral parameters (L, M, and O). n = 5 PR^{Cre} and 8 control females each for tests of pup retrieval and maternal aggression.

Data are represented as Mean ± SEM.

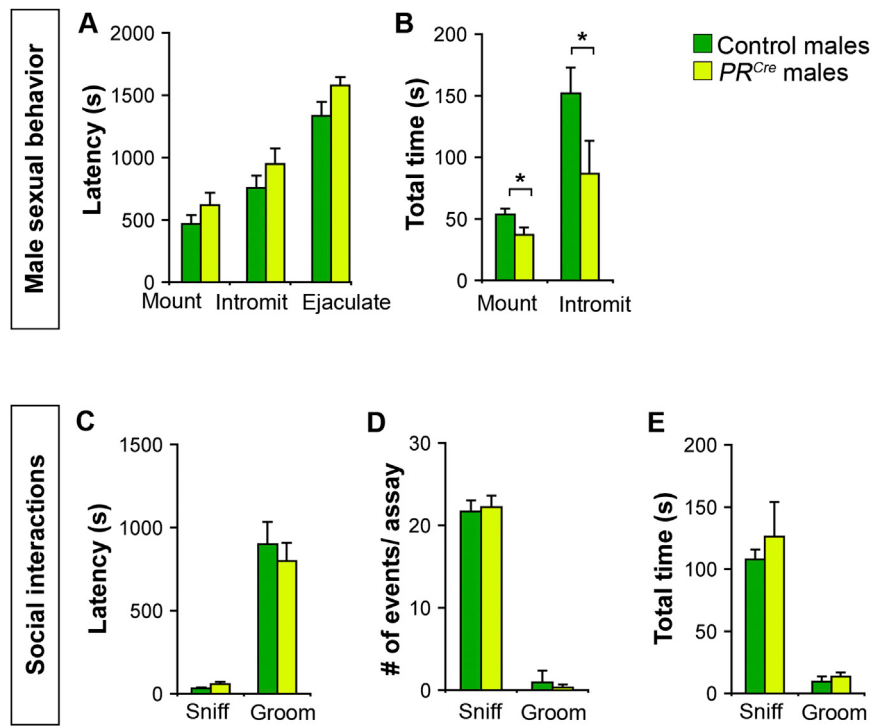


Figure S6. Males Lacking PR+ VMHvl Neurons Investigate Females Normally but Mate Less Often Than Controls, Related to Figure 6

Adult *PR^{Cre}* and control males were injected with AAV-flex-taCasp3-TEVp targeted to the VMHvl and tested for sexual behavior with WT estrus females.

(A) No difference between *PR^{Cre}* and control males in the latency to mount, intromit, or ejaculate.

(B) *PR^{Cre}* males spend less total time mounting and intromitting.

(C-E) No difference between *PR^{Cre}* and control males in sniffing or grooming females.

Mean \pm SEM; n \geq 24/experimental group; *, p < 0.05.

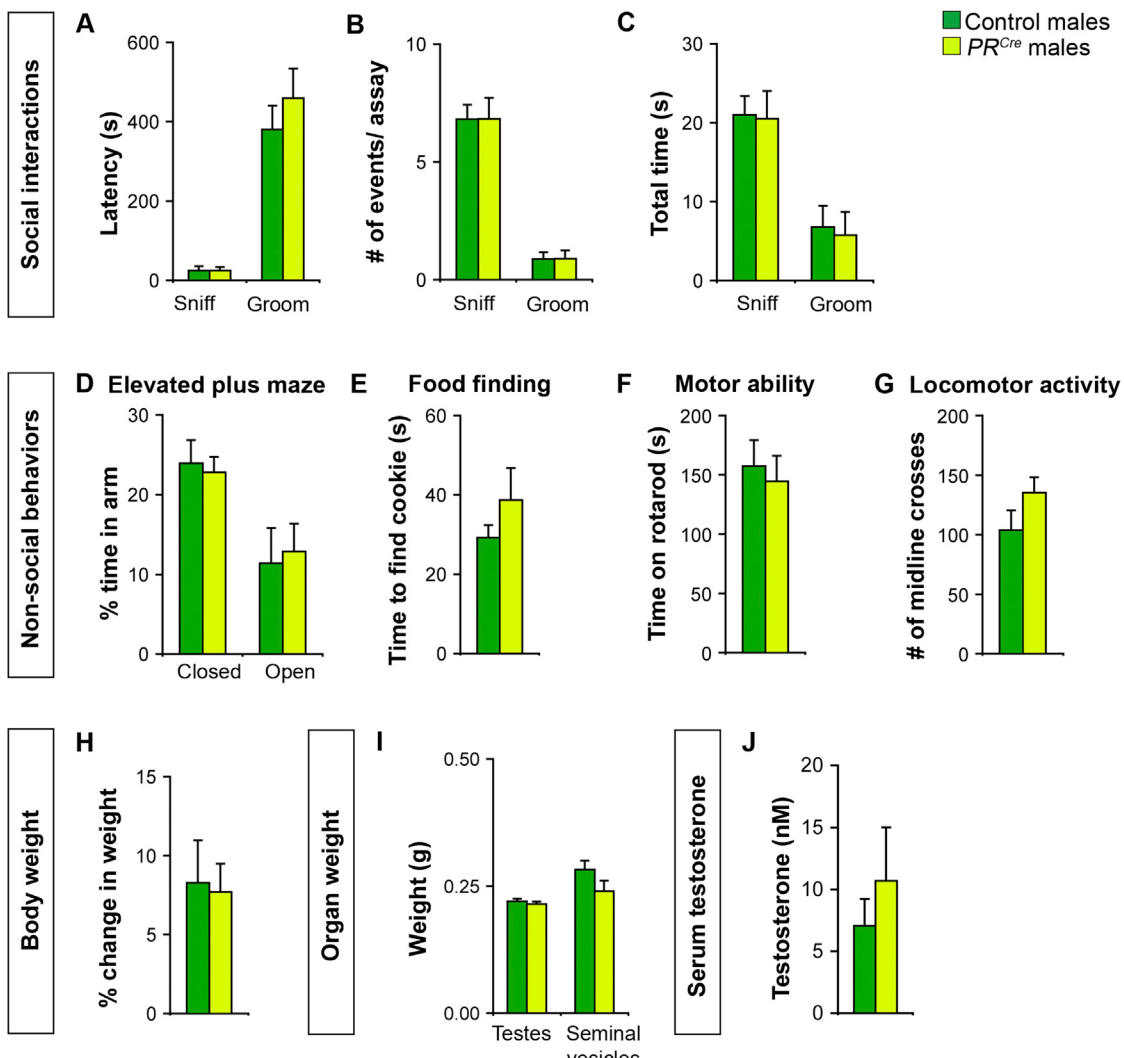


Figure S7. Males Lacking PR+ VMHvl Neurons Do Not Display Pervasive Deficits in Physiology or Behavior, Related to Figures 6 and 7

Adult PR^{Cre} and control males were injected with AAV-flex-taCasp3-TEVp targeted to the VMHvl and tested in different assays.

(A–C) No difference between PR^{Cre} and control males in sniffing or grooming intruder males. n ≥ 24/experimental group.

(D–G) No difference between PR^{Cre} and control males in tests of anxiety (D), motivation to find food (E), motor coordination and fatigue in the rotarod test (F), and general locomotor activity (G). n ≥ 11/experimental group.

(H) No difference between PR^{Cre} and control males in percent change in body weight 10 weeks following viral injection. n ≥ 11/experimental group.

(I) No difference between PR^{Cre} and control males in weight of testes or seminal vesicles. n ≥ 11/experimental group.

(J) No difference between PR^{Cre} and control males in serum testosterone titer. n = 13 /experimental group.

Data are represented as mean ± SEM.